isvr Institute of Sound and Vibration Research

Wave Reflection from Delaminations in Beams

A. Tassotti, B.R. Mace and T.P. Waters

ISVR Technical Memorandum No 953

August 2005

University of Southampton

SCIENTIFIC PUBLICATIONS BY THE ISVR

Technical Reports are published to promote timely dissemination of research results by ISVR personnel. This medium permits more detailed presentation than is usually acceptable for scientific journals. Responsibility for both the content and any opinions expressed rests entirely with the author(s).

Technical Memoranda are produced to enable the early or preliminary release of information by ISVR personnel where such release is deemed to the appropriate. Information contained in these memoranda may be incomplete, or form part of a continuing programme; this should be borne in mind when using or quoting from these documents.

Contract Reports are produced to record the results of scientific work carried out for sponsors, under contract. The ISVR treats these reports as confidential to sponsors and does not make them available for general circulation. Individual sponsors may, however, authorize subsequent release of the material.

UNIVERSITY OF SOUTHAMPTON

INSTITUTE OF SOUND AND VIBRATION RESEARCH

DYNAMICS GROUP

Wave Reflection from Delaminations in Beams

by

A. Tassotti, B.R. Mace and T.P. Waters

ISVR Technical Memorandum No: 953

August 2005

Authorised for issue by
Professor M.J. Brennan
Group Chairman

Contents

Abstract

The aim of this work is to estimate wave reflection and transmission coefficients for a delaminated composite beam. Those estimates can later be used in a wave-based method to detect the presence of the delamination. To calculate the values of the coefficients, the beam modelled using a Finite Element model of the delaminated region, connected with Spectral Element models of two semi-infinite beams one on either side of the delaminated section. Longitudinal and flexural waves are considered. The Spectral Element models have been developed for isotropic materials and for orthotropic laminate materials. Numerical results are presented, considering delaminations of various length and position between different layers, in order to investigate the relation between these parameters and the reflection and transmission coefficients.

Introduction

Composite materials are assuming growing importance in many industrial fields and in particular for aeronautical structures. Defects may be present in composite materials due to lack of accuracy during manufacturing or impacts and loads during service. These defects are usually inclusions of different materials, breakage of fibres and, for laminate composite structures, lack of connection between layers, called delamination. The presence of defects changes the mechanical properties of materials, in particular the local stiffness. As a consequence, during recent years many damage detection techniques have been developed, in order to investigate the presence of defects and to ensure the structural integrity of the material. Many damage detection techiques are based on changes in the dynamic behaviour of the structure, such as changes in natural frequencies, mode shapes, modal curvature,etc.

Recently, a damage detection technique based on wave propagation has been developed as a method to detect defects in beams ([1], [2], [3]). It is well known, in fact, that the presence of defects causes partial reflection of an incident wave; by measuring the reflection and transmission coefficients it is possible to detect the presence of irregularities in the structure.

This work contains the application of the cited method to delaminated, multilayered composite beams. First, reflection and transmission coefficients for isotropic and orthotropic laminate rods and beams are presented. Then the Spectral Element models are developed. In order to estimate the reflection and transmission coefficients of the delaminated beams a Finite Element model of the delaminated area is connected to two Spectral Element models of semi infinite beams, developed according to elementary rod theory, Love, Euler-Bernoulli and Timoshenko theories. Numerical results are then presented. We have considered delamination of various length and position between layers. The presence of the delamination is clearly visible comparing the reflection and transmission coefficients of the undamaged beam and

of the damaged beam. The numerical results are affected by the the non-perfect junction between Spectral Element models and the Finite Element model, but this effect is negligible if compared with the effect of the presence of the delamination.

Chapter 1

Wave propagation in rods and beams

1.1 General aspects

The propagation of waves is the consequence of an excitation on a structure: when a local disturbance occurs, it is transmitted to other positions of the medium in the form of waves which carry energy. These waves are called mechanical waves.

The aim of this chapter is to study wave propagation in elastic media with one-dimensional geometry (rods and beams), considering the following two types of waves:

- *Longitudinal waves*: the displacement of particles is parallel to the direction of wave propagation;
- *Transversal waves*: the displacement of particles is perpendicular to the direction of wave propagation.

First of all we consider isotropic material; secondly we study wave propagation in orthotropic laminated beam and rods.

1.2 Wave propagation in rods

1.2.1 Governing equation

The longitudinal wave motion in structures can be studied considering the rod shown in Fig.(1.1), subjected to a body force per unit volume $q(x,t)$.

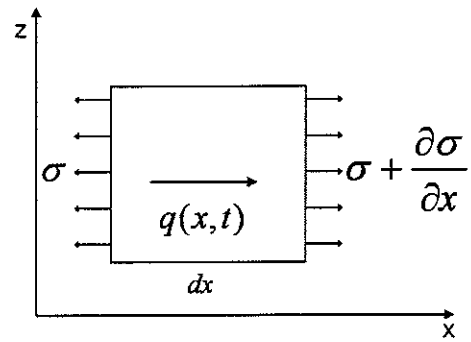

Figure 1.1: Differential element of the beam

It is possible, as in Reference [4], to write the equilibrium of a small element as

$$\frac{\partial \sigma}{\partial x} + q(x,t) = \rho \frac{\partial^2 u}{\partial t^2} \tag{1.1}$$

where $\sigma = \sigma(x)$ is a stress-field acting on the rod, ρ is the density of the material and u is the displacement in the x direction. According to Hooke's Law for isotropic materials $\sigma = E\epsilon$ and taking into account the strain-displacement relation $\epsilon = \partial u/\partial x$, equation (1.1) becomes

$$\frac{\partial^2 u}{\partial x^2} = \frac{1}{c_l^2} \frac{\partial^2 u}{\partial t^2} \tag{1.2}$$

where

$$c_l = \sqrt{\frac{E}{\rho}} \tag{1.3}$$

is the *phase velocity*. Equation (1.2) is the *longitudinal wave equation*. Since the phase velocity does not depend on the frequency, the wave motion is

called *nondispersive.*
If we assume an harmonic solution at frequency ω of the wave equation, $u(x,t) = U(x)e^{i\omega t}$, we find

$$\frac{d^2U(x,t)}{dx^2} + k_l^2 U = 0 \tag{1.4}$$

where the *wavenumber* is

$$k_l = \frac{\omega}{c_l} \tag{1.5}$$

and the *wavelength* (distance between two consecutive crests of a wave)

$$\lambda_l = \frac{2\pi}{k_l} \tag{1.6}$$

The total displacement, the sum of positive-going and negative-going propagating waves, can be written as

$$u(x,t) = C^+ e^{i(\omega t - k_l x)} + C^- e^{i(\omega t + k_l x)} \tag{1.7}$$

where C^+ and C^- are the wave amplitudes. The longitudinal force is

$$F = ES\frac{\partial u}{\partial x} \tag{1.8}$$

1.2.2 Group velocity

The expression for the positive-going propagating wave can be written as a sum of waves with different frequencies ω_i, wavenumbers and phase angles ϕ_i, i.e.

$$\sum_{i=1}^{n} C_i^+ \cos(\omega_i t - k_i x + \phi_i) \tag{1.9}$$

Now consider very small differences between two consecutive values of k_i and ω_i. At time t_0 and position x_0, we hypothesize that the differences between the phases of the wave components in the wave trains are very similar; the change in phase between the positions (t,x) and (t_o,x_o), where $t = t_0 + dt$ and $x = x_0 + dx$, is

$$dP_i = (\omega_i(t_0+dt) - k_i(x_0+dx) + \phi_i) - (\omega_i t_0 - k_i x_0 + \phi_i) = (\omega_i dt - k_i dx) \tag{1.10}$$

To maintain the wave group, the phase of two different wave components i and j has to be the same; this condition can be written as

$$dP_j - dP_i = 0 \tag{1.11}$$

which implies

$$(k_i - k_j)dx = (\omega_i - \omega_j)dt \tag{1.12}$$

It is possible to define the *group velocity* as

$$c_g = \frac{dx}{dt} = \frac{d\omega}{dk} \tag{1.13}$$

The phase velocity c is the speed at which a wave component of frequency ω propagates in the structure; the group velocity c_g is the speed at which the energy propagates. For a *nondispersive system* the group velocity equals the phase velocity; for a dispersive systems it is possible to have:

- $c > c_g$: the waves appear to originate at the rear of the group, travelling to the front and disappearing;
- $c = c_g$: there is no relative motion of the group;
- $c < c_g$: the waves appear to originate at the front of the group.

1.2.3 Reflection and transmission coefficients

A wave incident on a boundary or a discontinuity generates a reflected and a transmitted wave; their amplitudes and phases depend on the equilibrium and continuity conditions. We define the reflection and trasmission coefficents r and t as the ratios of the amplitudes of the reflected and transmitted waves to that of the incident wave.

The general aim of this work is to evaluate the presence of delamination by detecting reflected waves. The amplitude of these waves, which are determined by the reflection coefficients of the delamination, depend on the extent of damage. In order to apply this technique we evaluate the reflection and transmission coefficients for some simple examples in the following subsection.

Fixed end

If we consider a semi-infinite rod shown in Fig. (1.2), the displacement in x-direction $u(x,t)$ is

$$u(x,t) = C_i e^{i(\omega t - kx)} + C_r e^{i(\omega t + kx)} \tag{1.14}$$

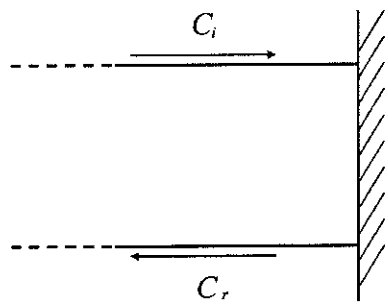

Figure 1.2: Rod with a fixed end

At the fixed end the displacement equals zero; if the origin of the coordinate system coincides with the end of the beam, we can write the boundary condition as

$$u(0,t) = C_i e^{i\omega t} + C_r e^{i\omega t} = 0 \tag{1.15}$$

and the reflection coefficent is

$$r = \frac{C_r}{C_i} = -1 \tag{1.16}$$

The incident wave is reflected by the fixed boundary with opposite sign.

Free end

The force at the position x and at the time t for a rod is

$$F(x,t) = ES\frac{\partial u}{\partial x} \tag{1.17}$$

where S is the cross section of the rod and E is the Young's modulus of the material. At the free end ($x = 0$) the force equals zero; the boundary condition can be written as

$$F(0,t) = ES\left(-ikC_i + ikC_r\right) \tag{1.18}$$

and the reflection coefficent is therefore

$$r = \frac{C_r}{C_i} = 1 \tag{1.19}$$

The incident wave is thus reflected by the fixed boundary, with the same sign.

Junction between two rods

Any kind of discontinuity reflects and transmits incident waves. We consider the junction between two semi-infinite rods 1 and 2, with different diameters and made up of two different materials (Fig. (1.3)).

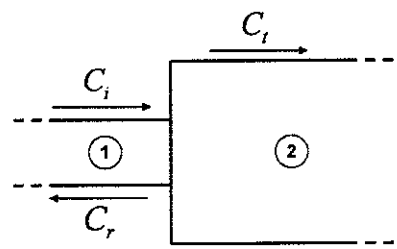

Figure 1.3: Junction between two different rods

In the left-hand rod there are incident and reflected waves, and transmitted waves propagate in the rod on the right-hand side; the axial displacements of the first and the second rod can be written as

$$\begin{aligned} u_1 &= C_i e^{i(\omega t - k_1 x)} + C_r e^{i(\omega t + k_1 x)} \\ u_2 &= C_t e^{i(\omega t - k_2 x)} \end{aligned} \tag{1.20}$$

where k_1 and k_2 are the wavenambers of the rods and C_i, C_r and C_t are the amplitudes of the incident, reflected and trasmitted waves. At the junction, equilibrium of forces $F_1 = F_2$ and continuity of displacement $u_1 = u_2$ give

$$\begin{aligned} F_i + F_r &= F_t \\ u_i + u_r &= u_t \end{aligned} \tag{1.21}$$

Substituting the expressions for the forces and displacements in the former equations we obtain

$$\begin{aligned} E_1 S_1 \left[k_1 C_i - k_1 C_r\right] &= E_2 S_2 k_2 C_t \\ C_i + C_r &= C_t \end{aligned} \tag{1.22}$$

The reflection and the transmission coefficients are then

$$\begin{aligned} r &= \frac{C_r}{C_i} = \frac{E_1 S_1 k_1 - E_2 S_2 k_2}{E_1 S_1 k_1 + E_2 S_2 k_2} \\ t &= \frac{C_t}{C_i} = \frac{2 E_1 S_1 k_1}{E_1 S_1 k_1 + E_2 S_2 k_2} \end{aligned} \tag{1.23}$$

From an analogy between electric and mechanic systems we can define the mechanical impedance as $Z_i = S_i \sqrt{\rho_i E_i}$; using the definition of the impedance, the coefficients may be written in the following forms

$$\begin{aligned} r &= \frac{Z_1 - Z_2}{Z_1 + Z_2} \\ t &= \frac{2 Z_1}{Z_1 + Z_2} \end{aligned} \tag{1.24}$$

Two rods with same Young's moduli and densities have same wavenumbers $k_1 = k_2 = k$; the coefficients depend only by the cross-sectional areas so that

$$\begin{aligned} r &= \frac{1 - \alpha}{1 + \alpha} \\ t &= \frac{2}{1 + \alpha} \end{aligned} \tag{1.25}$$

where $\alpha = \dfrac{S_2}{S_1}$ is the ratio of the cross-sectional areas.

1.3 Wave propagation in rods: Love theory

1.3.1 Governing equation

In the previous section we have considered the longitudinal rod theory, neglecting the Poisson effect, which causes transverse contractions and deflections due to axial displacement of the rod. Love rod theory considers these effects. According to Reference [5], the lateral displacements of a rod can

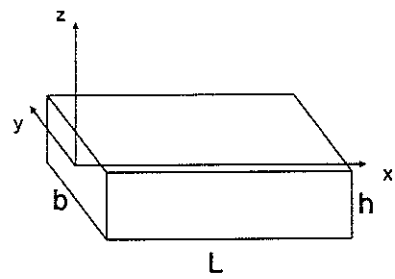

Figure 1.4: Dimensions of the considered rod

be written taking into account extension or contraction of the cross-section. Considering the isotropic rod shown in Fig (1.4) the displacements can be written as

$$\begin{aligned} u &= u(x) \\ v &= -\nu y u_{,x} \\ w &= -\nu z u_{,x} \end{aligned} \tag{1.26}$$

where u, v, w are the displacements along x, y and z axes, $u_{,x}$ is the first derivative of u respect to x and ν is the coefficient of Poisson of the material. The resulting strains and stresses are

$$\begin{aligned} \epsilon_{xx} &= u_{,x} \\ \sigma_{xx} &= E u_{,x} \end{aligned} \tag{1.27}$$

where E is the Young's modulus of the material.

We can obtain the equation of motion using the principle of virtual work. The variation of the strain energy can be written as

$$\delta\phi = \int_V \delta\epsilon_{xx}\sigma_{xx}dV = \int_0^L \left[\int_S (\delta u_{,x}\,\sigma_{xx}dS)\right] dx = [\delta u F]_0^L - \int_0^L \delta u F_{,x}\,dx \tag{1.28}$$

where $F = \int_S \sigma_{xx}dS$ is the longitudinal force and $F_{,x}$ is its first derivative with respect to x.

The variation of the internal work is

$$\delta W_{int} = -\int_V \rho\left[\delta u u_{,tt} + \delta v v_{,tt} + \delta w w_{,tt}\right] dV \tag{1.29}$$

Substituting equation (1.26) in this last, we obtain

$$\delta W_{int} = -\int_0^L \left[\int_S \rho\left(u_{,xtt}\,\delta u + \nu^2 y^2 u_{,xtt}\,\delta u_{,x} + \nu^2 z^2 u_{,xtt}\,\delta u_{,x}\right) dS\right] dx =$$

$$-\int_0^L \left[\rho S u_{tt}\delta u\right] dx - \left[\rho\nu^2 J u_{,xtt}\,\delta u\right]_0^L + \int_0^L \left[\rho\nu^2 J u_{,xxtt}\,\delta u\right] dx \tag{1.30}$$

where

$$J = \int_S \left(y^2 + z^2\right) dS \tag{1.31}$$

is the polar moment of the cross-sectional area S. If we equate the variation of the internal work and variation of strain energy we obtain

$$-F_{,x} = -\rho S\ddot{u} + \rho\nu^2 J^2 \ddot{u}_{,xx} \tag{1.32}$$

which can be written as

$$-ESu_{,xx} = -\rho S u_{tt} + \rho\nu^2 J^2 u_{,xxtt} \tag{1.33}$$

The final form of the equation of motion is

$$E\frac{\partial^2 u}{\partial x^2} = \rho\frac{\partial^2 u}{\partial t^2} - \frac{\rho\nu^2 J^2}{S}\frac{\partial^4 u}{\partial x^2 \partial t^2} \tag{1.34}$$

In the same way, considering the contribution due to contraction or extension of the cross-section, the longitudinal force is

$$F = ES\frac{\partial u}{\partial x} + \rho\nu^2 J^2 \frac{\partial}{\partial x}\left(\frac{\partial^2 u}{\partial t^2}\right) \tag{1.35}$$

Considering equations (1.34) and (1.35), we can notice that the result obtained using the Love rod theory is the same as simple rod theory (equations 1.2, 1.8) plus additional terms due to contraction, noticeable at high frequencies.

Assuming an harmonic solution of the form $u(x,t) = Ae^{i(\omega t - k_l x)}$ and substituting it into equation (1.34) we obtain the dispersion equation

$$-ESk_l^2 + \nu^2\rho J\left(k_l^2\omega^2\right) + \rho S\omega^2 = 0 \tag{1.36}$$

The wavenumber is

$$k_l = \sqrt{\frac{\rho S\omega^2}{ES - \nu^2\rho J\omega^2}} \tag{1.37}$$

Defining $k_0 = \omega\sqrt{\rho/E}$ and $k_r = \sqrt{S/J}$ we can write the wavenumber as

$$k_l = k_0\sqrt{\frac{1}{1 - \nu^2\left(k_o/k_r\right)^2}} \tag{1.38}$$

The general displacement can again be written as the sum of two wave components (see equation (1.7)).

1.4 Wave propagation in beams: Euler Bernoulli theory

1.4.1 Governing equation

Consider a differential element of the beam shown in Fig.(1.5)

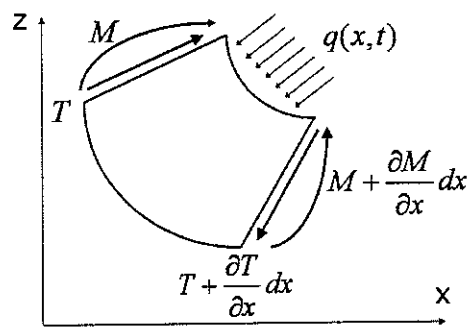

Figure 1.5: Differential element of the beam

As developed in Reference [4], the equilibrium of a differential element in the z direction, considering the body force per unit volume $q(x,t)$ and neglecting the effects of rotary inertia and shear deformation (*Euler-Bernoulli theory of the beam*), can be written as

$$\frac{\partial T}{\partial x} + q = -\rho S \frac{\partial^2 w}{\partial t^2} \tag{1.39}$$

If the body force $q(x,t)$ is zero, and substituting the shear-moment relation $T = \dfrac{\partial M}{\partial x}$, the last equation becomes

$$\frac{\partial^2 M}{\partial x^2} + \rho S \frac{\partial^2 w}{\partial x^2} = 0 \tag{1.40}$$

where w is the displacement in the x direction. The moment-displacement relation for the beam is

$$M = EI \frac{\partial^2 w}{\partial x^2} \tag{1.41}$$

where I is the *second moment of area* of the cross-section.Thus we obtain the equation of motion

$$\frac{\partial^4 w}{\partial x^4} + \frac{1}{a^2}\frac{\partial^2 w}{\partial x^2} = 0 \tag{1.42}$$

where

$$a^2 = \frac{EI}{\rho S} \tag{1.43}$$

For an *harmonic motion* with solution $w(x,t) = W(x)\, e^{i\omega t}$, equation (1.42) becomes

$$\frac{d^4 W}{dx^4} - k_{eb}^4 W = 0 \tag{1.44}$$

where the wavenumber is

$$k_{eb}^4 = \frac{\rho S \omega^2}{EI} \tag{1.45}$$

The general solution of equation (1.44) is

$$w(x,t) = A^+ e^{i(\omega t - k_{eb}x)} + A_n^+ e^{(i\omega t - k_{eb}x)} + A^- e^{i(\omega t + k_{eb}x)} + A_n^- e^{(i\omega t + k_{eb}x)} \tag{1.46}$$

The total displacement is the sum of positive and negative propagating travelling waves and positive and negative non propagating waves, called *nearfield waves*; these waves decay exponentially with distance and don't carry energy.

The phase velocity is

$$c_{eb} = \frac{\omega}{k_{eb}} = \sqrt[4]{\frac{EI}{\rho A}}\sqrt{\omega} \tag{1.47}$$

Since the phase velocity of the propagating waves depends on frequency, the wave motion is *dispersive*. The group velocity is

$$c_g = \frac{d\omega}{dk_{eb}} = 2\sqrt[4]{\frac{EI}{\rho A}}\sqrt{\omega} = 2c_{eb} \tag{1.48}$$

1.4.2 Reflection and transmission coefficients

As for the case of rods, we now find reflection and transmission coefficients for some examples.

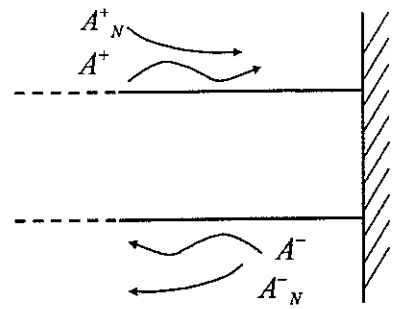

Figure 1.6: Beam with fixed end

Fixed end

We evaluate the reflection coefficient for the beam with a fixed end shown in Fig.(1.6); the boundary conditions, if the origin of the x-axis coincides with the fixed end, are

$$\begin{aligned} w(0,t) &= 0 \\ \frac{\partial w}{\partial x} &= 0 \end{aligned} \tag{1.49}$$

Referring to equation 1.46, solving the former system of equations, we obtain the *matrix of the reflection coefficients* $\mathbf{r}$ to be

$$\mathbf{r} = \begin{bmatrix} -i & -(i+1) \\ (i-1) & i \end{bmatrix} \tag{1.50}$$

where

$$\begin{Bmatrix} A^- \\ A^-_n \end{Bmatrix} = \mathbf{r} \begin{Bmatrix} A^+ \\ A^+_n \end{Bmatrix} \tag{1.51}$$

Free end

At a free end the moment and the shear force are equal to zero; the boundary conditions at the coordinate $(x = 0)$ can be written as

$$\frac{\partial^2 w}{\partial x^2} = 0$$
$$\frac{\partial^3 w}{\partial x^3} = 0 \tag{1.52}$$

The solution of the system of equations gives the matrix of the reflection coefficients

$$\mathbf{r} = \begin{bmatrix} i & (i-1) \\ (i+1) & -i \end{bmatrix} \tag{1.53}$$

where again

$$\begin{Bmatrix} A^- \\ A_n^- \end{Bmatrix} = \mathbf{r} \begin{Bmatrix} A^+ \\ A_n^+ \end{Bmatrix} \tag{1.54}$$

Junction between two semi-infinite beams

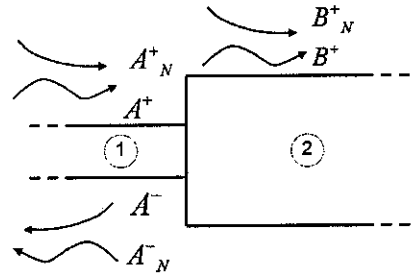

Figure 1.7: Juction between two semi-infinite beams

Referring to Fig.(1.7), we can write the displacements in the left and right- hand side beams as

$$w_1(x,t) = e^{i\omega t}\left[A^+ e^{-ik_1 x} + A^- e^{+ik_1 x} + A_n^+ e^{-k_1 x} + A_n^- e^{+k_1 x}\right]$$
$$w_2(x,t) = e^{i\omega t}\left[B^+ e^{-ik_2 x} + B_n^+ e^{-k_2 x} + A_n^- e^{+k_1 x}\right] \tag{1.55}$$

At the interface, the origin of the coordinate system, we write the following boundary conditions

- Continuity of displacement $w_1(0,t) = w_2(0,t)$
- Continuity of slope $\dfrac{\partial w_1(0,t)}{\partial x} = \dfrac{\partial w_2(0,t)}{\partial x}$
- Continuity of moment $EI_1 \dfrac{\partial^2 w_1(0,t)}{\partial x^2} = EI_2 \dfrac{\partial^2 w_2(0,t)}{\partial x^2}$
- Continuity of shear $EI_1 \dfrac{\partial^3 w_1(0,t)}{\partial x^3} = EI_2 \dfrac{\partial^3 w_2(0,t)}{\partial x^3}$

Solving the system of equations we obtain the following expressions

$$\begin{aligned} \mathbf{A}\mathbf{a}^+ + \mathbf{B}\mathbf{a}^- &= \mathbf{C}\mathbf{b}^+ \\ \mathbf{D}\mathbf{a}^+ + \mathbf{F}\mathbf{a}^- &= \mathbf{G}\mathbf{b}^+ \end{aligned} \tag{1.56}$$

where the vectors $\mathbf{a}^+ = \{A^+ A_n^+\}^T$, $\mathbf{b}^+ = \{B^+ B_n^+\}^T$ and $\mathbf{a}^- = \{A^- A_n^-\}^T$ contain the amplitudes of the positive and negative x-going waves and the matrices

$$\begin{aligned} \mathbf{A} &= \begin{bmatrix} 1 & 1 \\ i & 1 \end{bmatrix} \quad \mathbf{B} = \begin{bmatrix} 1 & 1 \\ -i & 1 \end{bmatrix} \quad \mathbf{C} = \begin{bmatrix} 1 & 1 \\ i\alpha^{1/2} & \alpha^{1/2} \end{bmatrix} \\ \mathbf{D} &= \begin{bmatrix} 1 & -1 \\ i & -1 \end{bmatrix} \quad \mathbf{E} = \begin{bmatrix} 1 & -1 \\ -i & 1 \end{bmatrix} \quad \mathbf{F} = \begin{bmatrix} 1 & 1 \\ i\alpha^{-5/2} & -\alpha^{-5/2} \end{bmatrix} \end{aligned} \tag{1.57}$$

Solving the given equations we evaluate the reflection and transmission coefficients; the results are complicated and are not given here.

1.5 Wave propagation in beams: Timoshenko theory

1.5.1 Governing equation

Formulating the Euler-Bernoulli theory for beams we neglected the effects of rotary inertia and shear deformation. As a consequence of these assumpions, the plane transversal section remains plane and perpendicular to the centroidal axis after the deformation. The Timoshenko beam theory considers these two terms, removing the limitations of the Euler-Bernoulli theory.

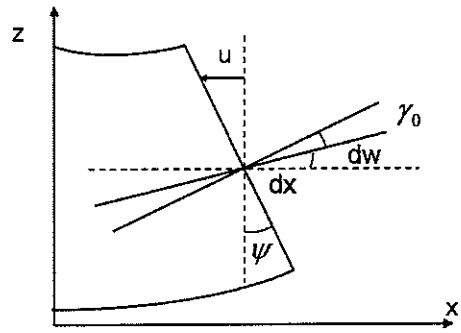

Figure 1.8: Shear effect

Referring to Fig.(1.8), we notice that now the slope of the centroidal axis $\partial w/\partial x$ is due to the effect of the bending ψ (angle of deflection of the cross section with respect to the vertical direction) and of the shear angle γ_0; it is possible to write

$$\frac{\partial w}{\partial x} = \psi - \gamma_0 \tag{1.58}$$

The contribution due to γ_0 can be calculate by the following relation between shear force and the shear strain:

$$T = G \int_S \gamma dS = G\gamma_0 S\kappa \tag{1.59}$$

where κ is the *Timoshenko shear coefficient.* The coefficient depends on the shape of the section. Using Equations (1.58) and (1.59) we obtain the shear force as

$$T = SG\kappa\left(-\frac{\partial w}{\partial x} + \psi\right) \tag{1.60}$$

where S is the area of the cross-section and G is the shear modulus of the isotropic material.

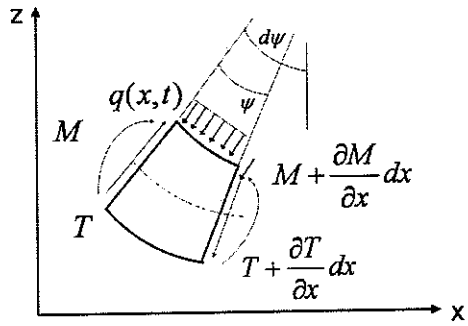

Figure 1.9: Differential element of the beam

If we consider the differential element of the beam shown in Fig.(1.9), we can write the equation of equilibrium along the z axis and the equation of equilibrium of the moment as

$$\frac{\partial T}{\partial x} + q = -\rho S dx \frac{\partial^2 w}{\partial t^2} \tag{1.61}$$

$$T - \frac{\partial M}{\partial x} = -\rho I \frac{\partial^2 \psi}{\partial t^2} \tag{1.62}$$

where I is the second moment of area of the beam. If we substitute equations (1.61) and (1.62) into the expression for the shear force (1.60) and the relation between the moment and the bending angle ψ, i.e. $M = EI\frac{\partial \psi}{\partial x}$, we obtain two *governing equations*

$$GS\kappa\left(\frac{\partial \psi}{\partial x} - \frac{\partial^2 w}{\partial x^2}\right) + \rho S \frac{\partial^2 w}{\partial t^2} = 0 \tag{1.63}$$

$$GS\kappa\left(\frac{\partial w}{\partial x}-\psi\right)+EI\frac{\partial^2\psi}{\partial x^2}=\rho I\frac{\partial^2\psi}{\partial t^2} \tag{1.64}$$

where the body force $q(x,t)=0$. These equation are coupled; we can reduce them to a single equation. The result is

$$\frac{EI}{\rho S}\frac{\partial^4 w}{\partial x^4}-\frac{I}{S}\left(1+\frac{E}{G\kappa}\right)\frac{\partial^4 w}{\partial x^2\partial t^2}+\frac{\partial^2 w}{\partial t^2}+\frac{\rho I}{GS\kappa}\frac{\partial^4 w}{\partial t^4}=0 \tag{1.65}$$

Considering a *time harmonic wave solution* of the equation of motion

$$w(x,t)=e^{i(\omega t-kx)} \tag{1.66}$$

we can obtain the dispersion equation

$$EIk^4-\rho I\left(1+\frac{E}{G\kappa}\right)\omega^2k^2-\rho S\omega^2+\frac{\rho^2 I}{G\kappa}\omega^4=0 \tag{1.67}$$

If we define

$$k_0=\omega\sqrt{\frac{\rho}{E}}\quad k_{eb}=\sqrt[4]{\frac{\rho S}{EI}}\sqrt{\omega}\quad k_s=\omega\sqrt{\frac{\rho}{G\kappa}} \tag{1.68}$$

equation (1.67) becomes

$$k^4-\left(k_0^2+k_s^2\right)k^2+\left(k_0^2k_s^2-k_{eb}^4\right) \tag{1.69}$$

Solving this equation we obtain two different wavenumbers: the first one (k_A) is a real number, the second one (k_B^*) is imaginary. We define, instead of calculated wavenumers, two real numbers k_A, which coincides with the real wavenumber k_A and k_B; the last one is the modulus of the imaginary wavenumber. These are given by

$$\begin{aligned}k_A&=\sqrt{\frac{\left(k_0^2+k_s^2\right)+\sqrt{\left(k_0^2+k_s^2\right)^2+4\left[k_{eb}^4+k_0^2k_s^2\right]}}{2}}\\ k_B&=\frac{k_B^*}{i}=\frac{1}{i}\sqrt{\frac{\left(k_0^2+k_s^2\right)-\sqrt{\left(k_0^2+k_s^2\right)^2-4\left[k_{eb}^4+k_0^2k_s^2\right]}}{2}}\end{aligned} \tag{1.70}$$

or

$$k_A = \sqrt{\frac{k_b^2}{2}\left(\left(\xi^2+\eta^2\right)+\sqrt{\left(\xi^2+\eta^2\right)^2+4\left(1+\xi^2\eta^2\right)}\right)}$$
$$k_B = \frac{1}{i}\sqrt{\frac{k_b^2}{2}\left(\left(\xi^2+\eta^2\right)-\sqrt{\left(\xi^2+\eta^2\right)^2+4\left(1+\xi^2\eta^2\right)}\right)} \tag{1.71}$$

where

$$\xi = k_0/k_b \quad \eta = k_s/k_b \tag{1.72}$$

The four roots of equation (1.69) are

$$k_1 = k_A \quad k_2 = -k_A$$
$$k_3 = ik_B \quad k_4 = -ik_B \tag{1.73}$$

and the general solutions of equations (1.63) and (1.64) can be written as

$$w(x,t) = e^{i\omega t}\left[A^+e^{-ik_Ax} + A^-e^{ik_Ax} + A_n^+e^{-k_Bx} + A_n^-e^{k_Bx}\right]$$
$$\psi(x,t) = e^{i\omega t}\left[R_AA^+e^{-ik_Ax} - R_AA^-e^{ik_Ax} + R_BA_n^+e^{-k_Bx} - R_BA_n^-e^{k_Bx}\right] \tag{1.74}$$

with

$$R_A = \frac{\kappa Gk_A^2 - \rho\omega^2}{\kappa Gik_A} \quad R_B = \frac{-\kappa Gk_B^2 - \rho\omega^2}{\kappa Gk_B} \tag{1.75}$$

The four wavenumbers show the presence of two pairs of wavemodes. In the low-frequency range, the values of the real wavenumber k_A is the same as the wavenumber calculated using Euler-Bernoulli theory for beams; the corresponding mode is a propagating mode. The imaginary wavenumber k_B^* corresponds to a nearfield wave. The imaginary wavenumber has a cutoff frequency above which it becomes a real number; the corresponding wavemode is propagating above this value of frequency.

1.6 Wave propagation in composite materials

1.6.1 Composite materials

Composite materials are made of two or more distinct materials, with different mechanical and physical properties or shapes, joined in order to obtain a new material with improved mechanical properties compared to those of the constituents. They are usually constituted by reinforcements (long and short fibers, particles, flakes,...) embedded in a metallic or polymeric matrix. Usually reinforcements carry loads and are bonded together by matrices. The principal advantages of composite materials are:

- high strength-to-weight ratio;
- corrosion and chemical resistance;
- tailoring.

Composite materials are usually obtained by joining some thin *laminae*; for fiber reinforced materials the *stacking sequence* determines the mechanical properties of the material. Multilayer composite structures are usually characterized by transversal anisotropic behaviour, large transversal deformability and high damage sensitivity: there is often some damage, such as breakage of fibers or the matrix and, in particular, the non-perfect connection between layers, called *delamination*. Defects in structures modify their mechanical behaviour and, therefore, wave propagation.

To study the effects of damage and delaminations in rods and beams, at first we modify, in the following subsections, the wave equation for rods and beams, taking into account the constitutive equations for orthotropic materials. The following analysis has been developed in [6]

1.6.2 Constitutive equations for orthotropic materials

The generalized Hooke's law, the relation between stress and strain components, can be written as

$$\sigma_{ij} = C_{ijkl}\epsilon_{kl} \tag{1.76}$$

where σ_{ij} is the ij stress component, ϵ_{kl} is the kl component of the strain and C_{ijkl} is the corresponding element of the stiffness matrix. The generalized

Hooke's law involves 21 independent coefficients; for orthotropic materials, if x, y, z are principle axes, it becomes

$$\begin{Bmatrix} \sigma_{xx} \\ \sigma_{yy} \\ \sigma_{zz} \\ \tau_{xz} \\ \tau_{yz} \\ \tau_{xy} \end{Bmatrix} = \begin{bmatrix} C_{11} & C_{12} & C_{13} & 0 & 0 & 0 \\ C_{12} & C_{22} & C_{23} & 0 & 0 & 0 \\ C_{13} & C_{23} & C_{33} & 0 & 0 & 0 \\ 0 & 0 & 0 & C_{44} & 0 & 0 \\ 0 & 0 & 0 & 0 & C_{55} & 0 \\ 0 & 0 & 0 & 0 & 0 & C_{66} \end{bmatrix} \begin{Bmatrix} \epsilon_{xx} \\ \epsilon_{yy} \\ \epsilon_{zz} \\ \gamma_{xz} \\ \gamma_{yz} \\ \gamma_{xy} \end{Bmatrix} \tag{1.77}$$

The coefficents C_{ij} in Eq. (1.6.2) are

$$C_{11} = E_1\frac{1-\nu_{23}\nu_{32}}{\Delta} \qquad C_{12} = E_1\frac{\nu_{21}+\nu_{31}\nu_{23}}{\Delta} = E_2\frac{\nu_{12}+\nu_{32}\nu_{13}}{\Delta}$$
$$C_{13} = E_1\frac{\nu_{31}+\nu_{21}\nu_{32}}{\Delta} = E_3\frac{\nu_{13}+\nu_{12}\nu_{23}}{\Delta} \qquad C_{22} = E_2\frac{1-\nu_{13}\nu_{31}}{\Delta}$$
$$C_{23} = E_2\frac{\nu_{32}+\nu_{12}\nu_{31}}{\Delta} = E_3\frac{\nu_{23}+\nu_{21}\nu_{13}}{\Delta} \qquad C_{33} = E_3\frac{1-\nu_{12}\nu_{21}}{\Delta} \tag{1.78}$$

$$C_{44} = G_{23} \quad C_{55} = G_{13} \quad C_{66} = G_{12} \tag{1.79}$$

with

$$\Delta = 1 - \nu_{12}\nu_{21} - \nu_{23}\nu_{32} - \nu_{31}\nu_{13} - 2\nu_{21}\nu_{32}\nu_{13} \tag{1.80}$$

where E_1, E_2, E_3 are the Young's moduli in the principal directions 1,2,3, ν_{ij} are the Poisson's ratios, and G_{23}, G_{13}, G_{12} are the shear moduli in the $2-3$, $1-3$ and $1-2$ planes.

Referring to the laminate fibre composite beam shown in Fig. (1.10), we can formulate the following hypothesis:

- we consider a *cross-ply* laminate, where ply orientation is 0^o or 90^o, in order to have only in-plane motion (i.e. loads in (x,y) plane generate deformations only in (x,y) plane);
- the laminate is symmetric. As a consequence, there is not bending-extensional coupling;
- if $b \approx h$, we can consider a *plane stress* condition.

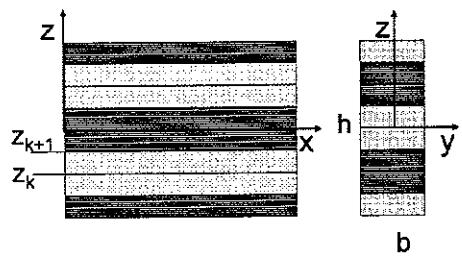

Figure 1.10: Composite beam

Because of the plane stress condition, the components of the stress τ_{yz}, τ_{xy}, σ_{yy} are very small. Since usually $\sigma_{xx} >> \sigma_{zz}$ and $\tau_{xz} >> \sigma_{zz}$, the significant stress components are σ_{xx} and τ_{xz}.

The initial assumpions lead to the stress-strain relation

$$\left\{ \begin{array}{c} \sigma_{xx} \\ \tau_{xz} \end{array} \right\} = \left[\begin{array}{cc} C_{11} & 0 \\ 0 & C_{44} \end{array} \right] \tag{1.81}$$

where the coefficients reduce to

$$C_{11} = E_{xx} \qquad C_{44} = G_{xz} \tag{1.82}$$

with $E_{xx} = E_1$ if $\vartheta = 0^o$ or $E_{xx} = E_2$ if $\vartheta = 90^o$ and, similarly, $G_{xz} = G_{13}$ or $G_{xz} = G_{23}$.

1.6.3 Laminate constitutive equations for orthotropic layers

We consider a laminate beam, built with N orthotropic laminae; in order to write the constitutive equations for laminate structures, we refers to the *First-Order Shera Deformation Theory* for laminate materials, as in Reference [6]. The FSDT is an *Equivalent Single-Layer* laminate theory, in which the laminate plate is reduced to an equivalent single-layer structure; it is based on the following hypotheses: the straight lines perpendicular to the midsurface

- remain straight after deformation;
- do not elongate during deformation;
- rotate, not remaining perpendicular to the midsurface after deformation.

According to the FSDT theory and taking into account the initial hypotheses, we can write the expressions for the longitudinal force F and for the moment M_y referring to the considered beam as

$$F = \int_A \sigma_{xx} dA = b \int_{-\frac{h}{2}}^{\frac{h}{2}} \sigma_{xx} dz = b \sum_{k=1}^{N} \int_{z_k}^{z_{k+1}} Q_{11}^k \left(\epsilon_x^0 + z\epsilon_x^1\right) dz \tag{1.83}$$

and

$$M_y = \int_S \sigma_{xx} dS = b \int_{-\frac{h}{2}}^{\frac{h}{2}} \sigma_{xx} z dz = b \sum_{k=1}^{N} \int_{z_k}^{z_{k+1}} Q_{11}^k \left(\epsilon_{xx}^0 + z\epsilon_{xx}^1\right) z dz \tag{1.84}$$

where ϵ_{xx}^0 are the *membrane strains* and ϵ_{xx}^1 are the *bending strains*, z_k and z_{k+1} are the coordinates in the z-direction of the interfaces of the considered layer and Q_{11}^k are the *plane stress-reduced stiffnesses* for each layer. The equations reduce to

$$F = b\left(A_{11}\epsilon_x^0 + B_{11}\epsilon_x^1\right) \tag{1.85}$$

$$M_y = b\left(B_{11}\epsilon_x^0 + D_{11}\epsilon_x^1\right) \tag{1.86}$$

Since the laminate is symmetric, the coupling term B_{11} between bending and extension is negligible and the coefficients A_{11} and D_{11} are

$$A_{11} = \sum_{k=1}^{N} Q_{11}^k \left(z_{k+1} - z_k\right) = \sum_{k=1}^{N} E_x^k \left(z_{k+1} - z_k\right) \tag{1.87}$$

$$D_{11} = \sum_{k=1}^{N} Q_{11}^k \frac{\left(z_{k+1}^3 - z_k^3\right)}{3} = \sum_{k=1}^{N} E_x^k \frac{\left(z_{k+1}^3 - z_k^3\right)}{3} \tag{1.88}$$

If we consider Timoshenko beam theory, the shear force along the z axis can be calculated as

$$T = \kappa \int_A \tau_{xz} dA = \kappa b \int_{-\frac{h}{2}}^{\frac{h}{2}} \tau_{xz} dz = \kappa b \int_{-\frac{h}{2}}^{h/2} \gamma_{xz} dz = b\kappa A_{44} \gamma_{xz} \tag{1.89}$$

where

$$A_{44} = \sum_{k=1}^{N} Q_{44}^k \left(z_{k+1} - z_k\right) = \sum_{k=1}^{N} G_{xz}^k \left(z_{k+1} - z_k\right) \tag{1.90}$$

1.6.4 Equations of motions for orthotropic laminated rods and beams

Rods

It is possible to write the equation of motion and expression for longitudinal force and the wavenumber for an orthotropic laminated rod. Referring to Fig.(1.1), the equilibrium of a differential element of a rod can be written, neglecting the body force, as

$$\frac{\partial F}{\partial x} = \rho S \frac{\partial^2 u}{\partial t^2} \tag{1.91}$$

where, for the beam shown in Fig. (1.10), the longitudinal force is

$$F = bA_{11} \frac{\partial u}{\partial x} \tag{1.92}$$

Equation (1.91) becames

$$\frac{\partial^2 u}{\partial x^2} = \frac{1}{c_l} \frac{\partial^2 u}{\partial t^2} \tag{1.93}$$

where the phase velocity is

$$c_l = \sqrt{\frac{bA_{11}}{\rho S}} \tag{1.94}$$

The displacements and stress/strain relations for the k-th layer can be written applying Love rod theory, as shown in section (1.3) for isotropic rods, i.e.

$$\begin{aligned} u &= u(x) \\ v &= -\nu_{12}^k y u_{,x} \\ w &= -\nu_{13}^k z u_{,x} \end{aligned} \tag{1.95}$$

$$\begin{aligned} \epsilon_{xx} &= u_{,x} \\ \sigma_{xx}^k &= E_x^k u_{,x} \end{aligned} \tag{1.96}$$

where E_x^k is the Young's modulus for each layer in the x direction. The variation of the strain energy is now

$$\delta\phi = \int_V \left[\delta\epsilon_{xx}\sigma_{xx}\right] dV = \left[\delta u F\right]_0^L - \int_0^L \delta u F_{,x}\, dx \tag{1.97}$$

and the variation of the internal work is

$$\begin{aligned} \delta W_{int} &= -\int_V \rho^k \left[u_{,tt}\,\delta u + v_{,tt}\,\delta v + w_{,tt}\,\delta w\right] dV = \\ &= -\int_0^L \left[\int_S \rho^k \left(u_{,tt}\,\delta u + \left(\nu_{12}^k\right)^2 y^2 u_{,xtt}\,\delta u_{,x} + \left(\nu_{13}^k\right)^2 z^2 u_{,xtt}\,\delta u_{,x}\right) dS\right] dx \end{aligned} \tag{1.98}$$

Defining

$$(\rho S)^* = \int_S \rho^k dS = b \int_{-h/2}^{h/2} \rho^k dz = b \sum_{k=1}^{N} \int_{z_k}^{z_{k+1}} \rho^k dz \tag{1.99}$$

and

$$(\rho J)^* = \int_S \left[\rho^k \left((\nu_{12}^k)^2 y^2 + (\nu_{13}^k)^2 z^2\right)\right] dS \tag{1.100}$$

we can write

$$\delta W_{int} = -\int_0^L \left[(\rho S)^* u_{,tt}\,\delta u\right] dx - \left[(\rho J)^* u_{,xtt}\,\delta u\right]_0^L + \int_0^L \left[(\rho J)^* u_{,xxtt}\,\delta u\right] dx \tag{1.101}$$

If we equate the variation of the internal work and the variation of the strain energy, the equation of motion can be written as

$$(E_x S)^* \frac{\partial^2 u}{\partial x^2} = (\rho S)^* \frac{\partial^2 u}{\partial t^2} - (\rho J)^* \frac{\partial^4 u}{\partial x^2 \partial t^2} \tag{1.102}$$

with

$$(E_x S)^* = \int_S E_x^k dS = b \int_{-h/2}^{h/2} E_x^k dz \tag{1.103}$$

The expression for the longitudinal force is now

$$F = (E_x S)^* \frac{\partial u}{\partial x} + (\rho J)^* \frac{\partial}{\partial x} \frac{\partial^2 u}{\partial t^2} \tag{1.104}$$

and the wavenumber is

$$k_l = \sqrt{\frac{(\rho S)^* \omega^2}{(E_x S)^* - (\rho J)^* \omega^2}} \tag{1.105}$$

Beams

The equilibrium of the beam element shown in Fig.(1.5), using equations (1.85) and (1.86), is

$$\frac{\partial^4 w}{\partial x^4} + \frac{1}{a^2} \frac{\partial^2 w}{\partial t^2} = 0 \tag{1.106}$$

where

$$a = \sqrt{\frac{bD_{11}}{\rho S}} \tag{1.107}$$

Using Timoshenko beam theory, equation (1.65) for an orthotropic laminate beam becomes

$$\frac{bD_{11}}{\rho S} \frac{\partial^4 w}{\partial x^4} - \frac{I}{S} \left(1 + \frac{S D_{11}}{\kappa A_{44} I} \right) \frac{\partial^4 w}{\partial x^2 \partial t^2} + \frac{\partial^2 w}{\partial t^2} + \frac{\rho I}{\kappa A_{44} b} \frac{\partial^4 w}{\partial t^4} = 0 \tag{1.108}$$

and, considering a time harmonic solution $w(x,t) = e^{i(\omega t - kx)}$ of the former equation, we find the wavenumbers to be

$$k_A = \sqrt{-\frac{\rho I}{bD_{11}}\left(1+\frac{SD_{11}}{\kappa A_{44} I}\right) + \sqrt{\left[\frac{\rho I}{bD_{11}}\left(1+\frac{SD_{11}}{\kappa A_{44} I}\right)\right]^2 + 4\left(\frac{\rho S\omega^2}{bD_{11}} - \frac{\rho^2 I S\omega^4}{\kappa A_{44} b^2 D_{11}}\right)}} \tag{1.109}$$

$$k_B = \sqrt{-\frac{\rho I}{bD_{11}}\left(1+\frac{SD_{11}}{\kappa A_{44} I}\right) - \sqrt{\left[\frac{\rho I}{bD_{11}}\left(1+\frac{SD_{11}}{\kappa A_{44} I}\right)\right]^2 + 4\left(\frac{\rho S\omega^2}{bD_{11}} - \frac{\rho^2 I S\omega^4}{\kappa A_{44} b^2 D_{11}}\right)}}/i \tag{1.110}$$

The coefficents R_A and R_B in equation (1.111) become

$$R_A = \frac{A_{44} b\kappa k_A^2 - \rho S\omega^2}{\kappa i k_A A_{44} b} \quad R_B = \frac{-A_{44} b\kappa k_B^2 - \rho S\omega^2}{\kappa A_{44} b k_B} \tag{1.111}$$

Chapter 2

The Spectral Element Method

2.1 General aspects of the Spectral Element Method

The most common tool we use to study the structural dynamics is the Finite Element Method. If the structure we are considering is very complicated, it is possible that the model will have a high number of degrees of freedom, needing a big computational effort. The Spectral Element Method allows to study wave propagation in structures directly in the frequency domain, obtaining the exact dynamic stiffness matrix of the element. Each beam is considered as a single element, and therefore the computational effort is very small; using the Spectral Element Method it is possible to remove some approximations of Finite Element Metod, because it uses exact shape functions and because there is not any discretization. These advantages are particularly important if we are considering an high frequencies. Complex structures can be studied as an assemblage of simple beam and rod elements. Doyle ([7]) has developed, for beams and rods, two elements: a two node element of finite length, and an element with one node, of infinite length, called throw-off element; the latter can transport energy out of the system. This element is usually used to model long beams, that usually require a high number of elements, when using a Finite Element model.

This chapter presents the spectral element for isotropic and orthotropic rods and beams.

2.2 Spectral Element Method for rods

2.2.1 Shape functions

To develop the Spectral Element Method for longitudinal waves it is necessary to calculate the shape functions of a given rod.

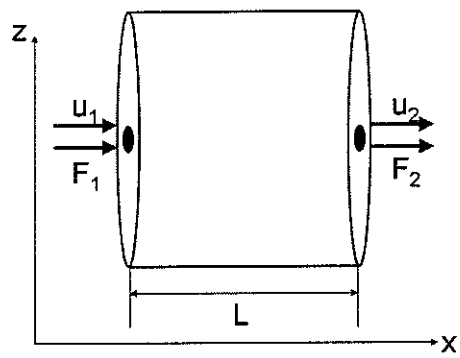

Figure 2.1: Rod element with two nodes

We consider the two-node rod element shown in Fig.(2.1) and we write the expression for the longitudinal displacement writing as a sum of positive and negative travelling waves. Suppressing the term $e^{i\omega t}$ it becomes

$$u(x) = C^{+}e^{-ikx} + C^{-}e^{-ik(L-x)} \tag{2.1}$$

where L is the length of the considered rod. If the values of the displacements at the ends of the rod are known, it is possible to determine the amplitudes of the positive and negative propagating waves C^{+} and C^{-} by solving the equations

$$u(0) = C^{+} + C^{-}e^{-ikL} = \widehat{u}_1 \tag{2.2}$$

$$u(L) = C^{+}e^{-ikL} + C^{-} = \widehat{u}_2 \tag{2.3}$$

Substituting the values of C^{+} and C^{-} in equation (2.1), we obtain

$$u(x) = g_1(x)\widehat{u}_1 + g_2(x)\widehat{u}_2 \tag{2.4}$$

where $g_1(x)$ and $g_2(x)$ are the frequency-dependent *shape functions* for the rod and are given by

$$g_1(x) = [e^{-ikx} - e^{-ik(2L-x)}]/\Delta \tag{2.5}$$

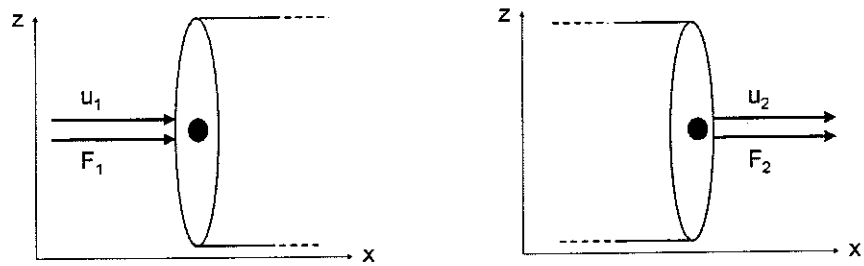

(a) Throw-off rod element-Left (b) Throw-off rod element-Right

Figure 2.2: Throw-off rod elements

$$g_2(x) = [-e^{-ikx} + e^{-ik(L-x)}]/\Delta \tag{2.6}$$

where

$$\Delta = [1 - e^{-2ikL}] \tag{2.7}$$

A single node element is one which extends to infinity in one direction. It is sometimes termed a semi-infinite or *throw-off* element and it conducts energy out of the system. For the throw-off element shown in Fig.(2.2), i.e. one which extends to $-\infty$, the longitudinal displacement, neglecting the $e^{i\omega t}$ term, assuming that there is no incident wave from $-\infty$,is given by

$$u(x) = C^{-}e^{ikx} \tag{2.8}$$

We impose the known value of the displacement on the node, i.e.

$$u(0) = C^{-} = \widehat{u}_2 \tag{2.9}$$

and the displacement can be rewritten using the shape function $g_2(x) = e^{ikx}$

$$u(x) = g_2(x)\,\widehat{u}_2 \tag{2.10}$$

For the left-hand side semi-infinite element shown in Fig.(2.2(b)), the displacement is

$$u(x) = g_1(x)\,\widehat{u}_1 \tag{2.11}$$

where the shape function is

$$g_1(x) = e^{-ikx} \tag{2.12}$$

2.2.2 Dynamic stiffness matrices

The internal force in the rod is given by

$$F(x) = ES\frac{\partial u}{\partial x} = ES[g_1'(x)\widehat{u}_1 + g_2'(x)\widehat{u}_2] \tag{2.13}$$

At the ends of the two-nodes rod element the forces are

$$F_1 = -F(0) = -ES[g_1'(0)\widehat{u}_1 + g_2'(0)\widehat{u}_2] \tag{2.14}$$

$$F_2 = F(L) = ES[g_1'(L)\widehat{u}_1 + g_2'(L)\widehat{u}_2] \tag{2.15}$$

Writing equations (2.14) and (2.15), in matrix form, we obtain the *dynamic stiffness matrix* $\mathbf{D}_l$ for the two-nodes rod element, i.e.

$$\left\{ \begin{array}{c} F_1 \\ F_2 \end{array} \right\} = ES \left[\begin{array}{cc} -g_1'(0) & -g_2'(0) \\ g_1'(L) & -g_2'(L) \end{array} \right] \left\{ \begin{array}{c} \widehat{u}_1 \\ \widehat{u}_2 \end{array} \right\} = \mathbf{D}_l \left\{ \begin{array}{c} \widehat{u}_1 \\ \widehat{u}_2 \end{array} \right\} \tag{2.16}$$

where

$$\mathbf{D}_l^+ = \mathbf{D}_l^+ = \frac{ikES}{1 - e^{-2ikL}} \left[\begin{array}{cc} 1 + e^{-2ikL} & -2e^{-ikL} \\ -2e^{-ikL} & 1 + e^{-2ikL} \end{array} \right] \tag{2.17}$$

In the same way we can calculate the dynamic stiffnes for both the throw-off elements to be

$$D_l^+ = D_l^- = ikES \tag{2.18}$$

For a laminate composite rod with rectangular cross-section, the dynamic stiffness for the throw-off elements, referring to Equation 1.87, are

$$D_l^+ = D_l^- = bA_{11}ik \tag{2.19}$$

2.2.3 Dynamic stiffness matrix: Love rod theory

According to the section (1.6.4), the dynamic stiffness matrix for both the throw-off orthotropic laminate rod elements, using Love rod theory, is

$$D_l^+ = D_l^- = (E_x S)^* ik - (\rho J)^* ik\omega^2 \tag{2.20}$$

referring to Equations 1.103 and 1.104.

2.3 Spectral Element Method for beams

2.3.1 Spectral Element Method using Euler-Bernoulli theory

As for the case of rods, to develop the Spectral Element Method for beams we write the expressions for displacement and rotation, using the Euler-Bernoulli theory, as

$$w(x) = A^{+}e^{-ikx} + A_n^{+}e^{-kx} + A^{-}e^{-ik(L-x)} + A_n^{-}e^{-k(L-x)}$$

$$\phi(x) = \frac{\partial w}{\partial x} = -ikA^{+}e^{-ikx} - kA_n^{+}e^{-kx} + ikA^{-}e^{-ik(L-x)} + kA_n^{-}e^{-k(L-x)} \tag{2.21}$$

Using vector notation

$$\left\{ \begin{array}{c} w(x) \\ \phi(x) \end{array} \right\} = \left\{ \begin{array}{c} g(x) \\ dg(x)/dx \end{array} \right\} \mathbf{A} \tag{2.22}$$

where

$$g(x) = \left\{ \begin{array}{cccc} e^{-ikL} & e^{-kL} & e^{-ik(L-x)} & e^{-k(L-x)} \end{array} \right\} \tag{2.23}$$

and the vector of wave amplitudes is

$$\mathbf{A} = \left\{ \begin{array}{cccc} A^{+} & A_n^{+} & A^{-} & A_n^{-} \end{array} \right\}^T \tag{2.24}$$

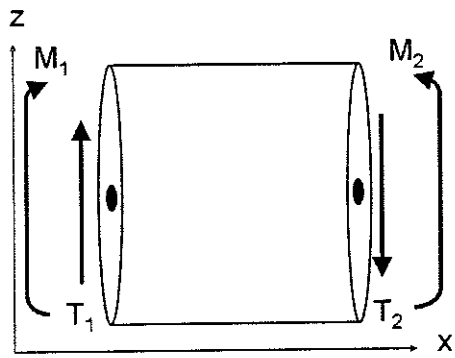

Figure 2.3: Two nodes beam element

Referring to Fig.(2.3), we apply the boundary conditions at the two nodes to get

$$\begin{aligned} w(0) &= A^+ + A_n^+ + A^- e^{-ikL} + A_n^- e^{-kL} = \widehat{w}_1 \\ \phi(0) &= -ikA^+ - kA_n^+ + ikA_n^- + kA_n^- = \widehat{\phi}_1 \\ w(L) &= A^+ e^{-ikL} + A_n^+ e^{-kL} + A^- + A_n^- = \widehat{w}_2 \\ \phi(L) &= -ikA^+ e^{-ikL} - kA_n^+ e^{-kL} + ikA_n^- + kA_n^- = \widehat{\phi}_2 \end{aligned} \tag{2.25}$$

Writing the former equations in matrix form we obtain

$$\begin{bmatrix} 1 & 1 & e^{-ikL} & e^{-kL} \\ -ik & -k & ike^{-ikL} & ke^{-kL} \\ e^{-ikL} & e^{-kL} & 1 & 1 \\ -ike^{-ikL} & -ke^{-kL} & ik & k \end{bmatrix} \begin{bmatrix} A^+ \\ A_n^+ \\ A^- \\ A_n^- \end{bmatrix} = \begin{bmatrix} \widehat{w}_1 \\ \widehat{\phi}_1 \\ \widehat{w}_2 \\ \widehat{\phi}_2 \end{bmatrix} \tag{2.26}$$

or

$$\mathbf{GA} = \widehat{\mathbf{w}} \tag{2.27}$$

The forces $\mathbf{F} = \{T_1 M_1 T_2 M_2\}^T$ at the ends of the beam of length L are calculated knowing the internal forces T, M at the given positions $x = 0$ and $x = L$, according to the given coordinate system and are

$$\begin{Bmatrix} T_1 \\ M_1 \\ T_2 \\ M_2 \end{Bmatrix} = \begin{Bmatrix} T(0) \\ M(0) \\ -T(L) \\ M(L) \end{Bmatrix} = EI \begin{Bmatrix} g'''(x) \\ g''(x) \\ -g'''(x) \\ g''(x) \end{Bmatrix} \mathbf{A} = EI \begin{Bmatrix} g'''(x) \\ g''(x) \\ -g'''(x) \\ g''(x) \end{Bmatrix} \mathbf{G}^{-1} \widehat{\mathbf{w}} \tag{2.28}$$

The matrix form is

$$\begin{Bmatrix} T_1 \\ M_1 \\ T_2 \\ M_2 \end{Bmatrix} = EI \begin{bmatrix} ik^3 & -k^3 & -ik^3 e^{-ikL} & k^3 e^{-kL} \\ k^2 & -k^2 & k^2 e^{-ikL} & -k^2 e^{-kL} \\ -ik^3 e^{-ikL} & +k^3 e^{-kL} & ik^3 & -k^3 \\ -k^2 e{-ikL} & k^2 e^{-kL} & -k^2 & k^2 \end{bmatrix} \mathbf{G}^{-1} \widehat{\mathbf{w}} \tag{2.29}$$

It is straightforward but tedius find an analytical expression for the dynamic stiffness matrix $\mathbf{D}_f$, which can be written as

$$\mathbf{F} = \mathbf{D}_f \widehat{\mathbf{w}} \tag{2.30}$$

where $\mathbf{F}$ is the vector of forces, $\widehat{\mathbf{w}}$ is the vector of displacements and rotation and the dynamic stiffness matrix for flexural waves is

$$\mathbf{D}_f = EI \begin{Bmatrix} g'''(x) \\ g''(x) \\ -g'''(x) \\ g''(x) \end{Bmatrix} \mathbf{A} = EI \begin{Bmatrix} g'''(x) \\ g''(x) \\ -g'''(x) \\ g''(x) \end{Bmatrix} \mathbf{G}^{-1} \tag{2.31}$$

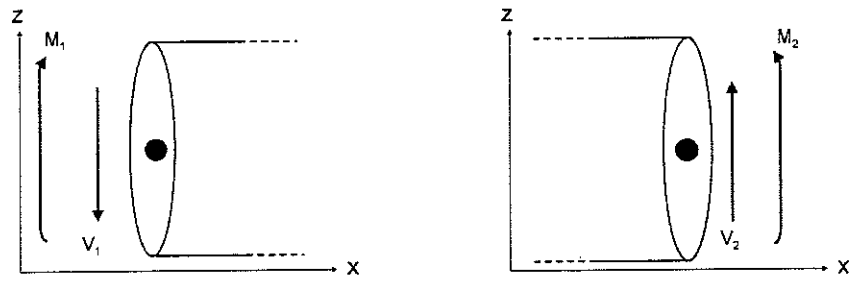

(a) Throw-off beam element-Left (b) Throw-off beam element-Right

Figure 2.4: Throw-off beam elements

In the same way, referring to the throw-off element shown in Fig.(2.4(a)), the displacement and rotation can be written as

$$\begin{aligned} w(x) &= A^+ e^{-ikx} + A_n^+ e^{-kx} \\ \phi(x) &= \frac{\partial w}{\partial x} = -ikA^+ e^{-ikx} - kA_n^+ e^{-kx} \end{aligned} \tag{2.32}$$

The boundary conditions can be written as

$$\begin{aligned} w(0) &= A^+ + A_n^+ = \widehat{w}_1 \\ \phi(0) &= -ikA^+ - kA_n^+ = \widehat{\phi}_1 \end{aligned} \tag{2.33}$$

It is possible to calculate the coefficients A^+ and A_n^+ and therefore the shape functions of the Euler-Bernoulli semi infinite element. They are given by

$$w(x) = \frac{(i+1)}{2} \left[e^{-ikx} - ie^{-kx}\right] \widehat{w}_1 + \frac{(i+1)}{2k} \left[e^{-ikx} - ie^{-kx}\right] \widehat{\phi}_1 \tag{2.34}$$

From the displacement, we can write the forces on the end of the beam, to obtain the dynamic stiffness matrix

$$\left\{ \begin{array}{c} \widehat{T}_1 \\ \widehat{M}_1 \end{array} \right\} = EI \left[\begin{array}{cc} (i-1)k^3 & ik^2 \\ ik^2 & (i+1)k \end{array} \right] \left\{ \begin{array}{c} \widehat{w}_1 \\ \widehat{\phi}_1 \end{array} \right\} \tag{2.35}$$

or

$$\mathbf{F} = \mathbf{D}_f^+ \widehat{\mathbf{w}} \tag{2.36}$$

where $\mathbf{F} = \left\{ \widehat{T}_1 \ \widehat{M}_1 \right\}^T$, $\mathbf{w} = \widehat{\left\{ \widehat{w}_1 \widehat{\phi}_1 \right\}^T}$

The dynamic stiffness matrix for the semi infinite element extending to $-\infty$, shown in Fig. 2.4(b)beam on the left-hand side is found in a similar way to be

$$\mathbf{D}_f^- = EI \left[\begin{array}{cc} (i-1)k^3 & -ik^2 \\ -ik^2 & (i+1)k \end{array} \right] \tag{2.37}$$

For a laminate orthotropic semi-infinite beam with rectangular cross-secton, the dynamic stiffness matrices become

$$\mathbf{D}_f^+ = bD_{11} \left[\begin{array}{cc} (i-1)k^3 & ik^2 \\ ik^2 & (i+1)k \end{array} \right] \tag{2.38}$$

$$\mathbf{D}_f^- = bD_{11} \left[\begin{array}{cc} (i-1)k^3 & -ik^2 \\ -ik^2 & (i+1)k \end{array} \right] \tag{2.39}$$

referring to Equation 1.88.

2.3.2 Spectral Element Method: Timoshenko beam

Shape functions for the semi-infinite beams

Referring to the beam shown in Fig.(2.4(a)), the displacement and rotation, using Timoshenko theory, are

$$\begin{aligned} w(x) &= A^{+}e^{-ik_A x} + A_n^{+}e^{-k_B x} \\ \psi(x) &= R_A A^{+}e^{-ik_A x} + R_B A_n^{+}e^{-k_B x} \end{aligned} \tag{2.40}$$

where k_A, k_B, R_A and R_B are given in Equations 1.109, 1.110, 1.111. We impose the boundaries conditions

$$\begin{aligned} w(0) &= A^{+} + A_n^{+} = \widehat{w}_1 \\ \psi(0) &= R_A A^{+} + R_B A_n^{+} = \widehat{\psi}_1 \end{aligned} \tag{2.41}$$

Solving for the constants A^{+} and A_n^{+}, equations (2.40) can be now written as

$$\begin{aligned} w(x) &= g_{w_1}\widehat{w}_1 + g_{w_2}\widehat{\psi}_1 \\ \psi(x) &= g_{\psi_1}\widehat{w}_1 + g_{\psi_2}\widehat{\psi}_1 \end{aligned} \tag{2.42}$$

where the *shape functions* are

$$\begin{aligned} g_{w1} &= \frac{1}{\Delta}\left[-R_B e^{-ik_A x} + R_A e^{-k_B x}\right] \\ g_{w2} &= \frac{1}{\Delta}\left[e^{-ik_A x} - e^{-k_B x}\right] \\ g_{\psi 1} &= \frac{1}{\Delta}\left[-R_A R_B e^{-ik_A x} + R_A R_B e^{-k_B x}\right] \\ g_{\psi 2} &= \frac{1}{\Delta}\left[R_A e^{-ik_A x} - R_B e^{-k_B x}\right] \end{aligned} \tag{2.43}$$

and where $\Delta = R_A - R_B$. The shear force and the moment are

$$T = GS\kappa\left(\psi - \frac{\partial w}{\partial x}\right)$$
$$M = EI\frac{\partial \psi}{\partial x} \tag{2.44}$$

Calculating the internal forces at the end of the element, we find that the dynamic stiffness matrix for the beam is such that

$$\left\{ \begin{array}{c} T_1 \\ M_1 \end{array} \right\} = \left\{ \begin{array}{c} T(0) \\ M(0) \end{array} \right\} = \mathbf{D}_f^+ \widehat{\mathbf{w}} \tag{2.45}$$

where

$$\mathbf{D}_f^+ = \frac{1}{\Delta}\left[\begin{array}{cc} GS\kappa\left(k_B R_A - ik_A R_B\right) & GS\kappa\left(ik_A + R_A - k_B - R_B\right) \\ EI\left(R_A R_B k_B - iR_A R_B k_A\right) & EI\left(iR_A k_A - R_B k_B\right) \end{array} \right] \left\{ \begin{array}{c} w_1 \\ \psi_1 \end{array} \right\}$$

(2.46)

For the throw-off beam shown in Fig.(2.4(b)) we have

$$w(x) = C^- e^{ik_A x} + C_n^- e^{k_B x}$$
$$\psi(x) = -R_A C^- e^{ik_A x} - R_B C_n^- e^{k_B x} \tag{2.47}$$

At the origin of the coordinate system, the displacement and rotation are

$$w(0) = C^- + C_n^- = \widehat{w}_1$$
$$\psi(0) = -R_A C^- - R_B C_n^- = \widehat{\psi}_1 \tag{2.48}$$

The shape functions are now

$$
\begin{aligned}
g_{w1} &= \frac{1}{\Delta}\left[-R_B e^{ik_A x} + R_A e^{k_B x}\right] \\
g_{w2} &= \frac{1}{\Delta}\left[-e^{ik_A x} + e^{k_B x}\right] \\
g_{\psi 1} &= \frac{1}{\Delta}\left[R_A R_B e^{ik_A x} - R_A R_B e^{k_B x}\right] \\
g_{\psi 2} &= \frac{1}{\Delta}\left[R_A e^{ik_A x} - R_B e^{k_B x}\right]
\end{aligned}
\tag{2.49}
$$

The vector of the forces for the semi-infinite beam is then

$$
\left\{ \begin{array}{c} T_1 \\ M_1 \end{array} \right\} = \left\{ \begin{array}{c} -T(0) \\ M(0) \end{array} \right\} = \widehat{\mathbf{D}}_f^- \left\{ \begin{array}{c} w_1 \\ \psi_1 \end{array} \right\} \tag{2.50}
$$

with

$$
\widehat{\mathbf{D}}_f^- = \frac{1}{\Delta}\left[\begin{array}{ll} GS\kappa\left(k_B R_A - ik_A R_B\right) & GS\kappa\left(k_B + R_B - ik_A - R_A\right) \\ EI\left(ik_A R_A R_B - k_B R_A R_B\right) & EI\left(ik_A R_A - k_B R_B\right) \end{array} \right] \tag{2.51}
$$

Referring to subsection (1.6.3), the dynamic stiffness matrices for laminate orthotropic semi-infinite beams are

$$
\mathbf{D}_f^+ = \frac{1}{\Delta}\left[\begin{array}{ll} A_{44} b\kappa\left(k_B R_A - ik_A R_B\right) & A_{44} b\kappa\left(ik_A + R_A - k_B - R_B\right) \\ bD_{11}\left(R_A R_B k_B - iR_A R_B k_A\right) & bD_{11}\left(iR_A k_A - R_B k_B\right) \end{array} \right] \tag{2.52}
$$

$$
\widehat{\mathbf{D}}_f^- = \frac{1}{\Delta}\left[\begin{array}{ll} A_{44} b\kappa\left(k_B R_A - ik_A R_B\right) & A_{44} b\kappa\left(k_B + R_B - ik_A - R_A\right) \\ bD_{11}\left(ik_A R_A R_B - k_B R_A R_B\right) & bD_{11}\left(ik_A R_A - k_B R_B\right) \end{array} \right] \tag{2.53}
$$

Chapter 3

Estimation of reflection and transmission coefficients using the SE Method

3.1 General aspects

As shown in the first chapter, the presence of discontinuities such as a change in section of the beam causes a partial reflection of the propagating wave. The presence of a defect in the structure also causes a partial reflection and transmission of the incident wave; this characteristic can be used to infer the presence of defects. The aim of this chapter is to apply a damage detection method which is able to detect the presence of delaminations in composite orthotropic laminated beams,by estimating the reflection and transmission coefficients due to the presence of defects. It is well known that, for an infinite rod without any defect or discontinuity, the reflection coefficient is zero and the transmission coefficient is one, because the incident wave is totally trasmitted. Any deviation from these values is an indication of the presence of some discontinuities or damage. The method, developed by Shone et al.([1], [?]) models the damaged infinite beam using a Finite Element model of the delaminated area, jointed at the left-hand side and at the right-hand side to two semi-infinite beams, modelled by Spectral Element Method.

3.2 Condensed dynamic stiffness matrix-FE model

3.2.1 Dynamic stiffness matrix for the damaged area

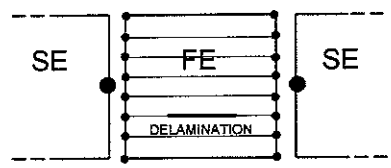

Figure 3.1: Model of the beam with SEs and FE

We model the damaged area of the beam shown in Fig.(3.1) using a finite elemente model. There is a delamination between two layers of the beam. It is assumed that the considered laminate is symmetric, so that there is no coupling between bending and torsion. The dynamic stiffness matrix of the beam can be calculated, if we know the mass and stiffness matrices $\mathbf{M}$ and $\mathbf{K}$, as

$$\mathbf{D} = \mathbf{K} - \omega^2 \mathbf{M} \tag{3.1}$$

If we assume that external forces are applied only at the nodes on the left-hand side and right-hand side of the FE modelled region, we can partition the matrix into elements associated with the boundary and the internal degrees of freedom. If $\phi_\mathbf{b}$ and $\phi_\mathbf{i}$ are the vectors of boundary and the internal degrees of freedom and $\mathbf{f_b}$ is the vector of the external forces on the boundaries, the partition of the dynamic stiffness matrix can be written as

$$\begin{Bmatrix} \mathbf{f_b} \\ \mathbf{0} \end{Bmatrix} = \begin{bmatrix} \mathbf{D}_{bb} & \mathbf{D}_{bi} \\ \mathbf{D}_{ib} & \mathbf{D}_{ii} \end{bmatrix} \begin{Bmatrix} \phi_b \\ \phi_i \end{Bmatrix} \tag{3.2}$$

By writing the second row to dirimate $\phi_\mathbf{i}$, it is possible to obtain the *condensed dynamic stiffness matrix* $\mathbf{D}_{FE}$ as

$$\mathbf{f_b} = \left[\mathbf{D}_{bb} - \mathbf{D}_{bi} \cdot \mathbf{D}_{ii}^{-1} \cdot \mathbf{D}_{ib}\right] \cdot \phi_b = \mathbf{D}_{FE} \cdot \phi_b \tag{3.3}$$

3.2.2 Reduction of the nodes and of the DOFs

To join the models of the two semi-infite beams with the model of the delaminated region, it is necessary to reduce the degrees of freedoms of the FE model by writing equilibrium and compatibily equations at the junction between the SE and the FE models. The semi-infinite beams present a single-node with three degrees of freedom (translation in the x direction, u, translation in the z direction, w and rotation φ around the y axis). The FE model has D nodes on each face and a various number of degrees of freedom for each node, depending on the element we have used to mesh the beam. In order to explain the method, we consider an element with two degrees of freedom per node (u and w). Referring to Fig.(3.2), we can write equation for the reduction of the degrees of freedom. For a generic node i of the FE model, the nodal displacements are related to those of the SE by

$$\begin{cases} u_i^L = u^L - \varphi^L z_i \\ w_i^L = w^L \end{cases} \qquad (3.4)$$

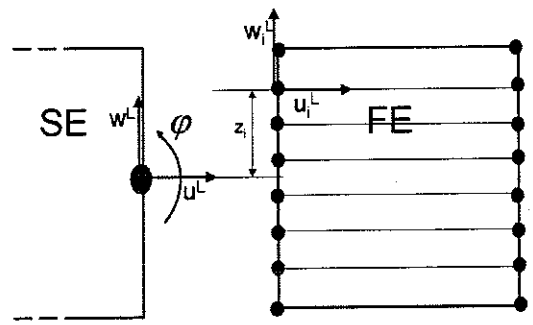

Figure 3.2: Reduction of the degrees of freedom

where z_i the coordinate of the node i in the z direction (the origin of the local coordinate system is on the mid-plane of the beam and coincides with the node of the SE). We can write the former equations using matrices as

$$\left\{ \begin{array}{c} u_i^L \\ w_i^L \end{array} \right\} = \left[\begin{array}{ccc} 1 & 0 & -z_i \\ 0 & 1 & 0 \end{array} \right] \left\{ \begin{array}{c} u^L \\ w^L \\ \varphi^L \end{array} \right\} = \mathbf{T}_i^L \phi^{\mathbf{L}} \tag{3.5}$$

For the right-hand face we can write the same equations, i.e.

$$\left\{ \begin{array}{c} u_i^R \\ w_i^R \end{array} \right\} = \left[\begin{array}{ccc} 1 & 0 & -z_i \\ 0 & 1 & 0 \end{array} \right] \left\{ \begin{array}{c} u^R \\ w^R \\ \varphi^R \end{array} \right\} = \mathbf{T}_i^R \phi^{\mathbf{R}} \tag{3.6}$$

The complete system of equations is formed by assembling equations 3.5 and 3.6 for all nodes and is

$$\phi_{FE} = \mathbf{T} \phi_{SE} \tag{3.7}$$

where the vector of the degrees of freedom of the FE and of the SE models are

$$\phi_{FE} = \left\{ \begin{array}{cccccccccccccc} u_1^L & w_1^L & u_2^L & w_2^L & \ldots & u_D^L & w_D^L & u_1^R & w_1^R & u_2^R & w_2^R & \ldots & u_D^R & w_D^R \end{array} \right\}^T \tag{3.8}$$

$$\phi_{SE} = \left\{ \begin{array}{cccccc} u^L & w^L & \varphi^L & u^R & w^R & \varphi^R \end{array} \right\} \tag{3.9}$$

The complete transformation matrix is then

$$\mathbf{T} = \left[\begin{array}{cc} \mathbf{T}_1^L & \mathbf{0} \\ \mathbf{T}_2^L & \mathbf{0} \\ \ldots & \ldots \\ \mathbf{T}_D^L & \mathbf{O} \\ \mathbf{0} & \mathbf{T}_1^R \\ \mathbf{0} & \mathbf{T}_2^R \\ \ldots & \ldots \\ \mathbf{0} & \mathbf{T}_D^R \end{array} \right] \tag{3.10}$$

where $\mathbf{0}$ is a matrix of zeros or appropriate size.

The *condensed dynamic stiffness matrix is*

$$\mathbf{D}_{FFE} = \mathbf{T}^T \cdot \mathbf{D}_{FE} \cdot \mathbf{T} \tag{3.11}$$

where $\mathbf{D}_{FE}$ is a $2D$ by $2D$ matrix and $\mathbf{D}_{FFE}$ is a 6 by 6 matrix.

3.3 Assembling the FE and SE models

To assemble SE and FE models, we first form the dynamic stiffness matrices for the spectral elements $\mathbf{D}^+$ and $\mathbf{D}^-$ on the left-hand side and the right-hand side of the FE model for longitudinal and flexural waves, i.e.

$$\mathbf{D}^+ = \begin{bmatrix} D_l^+ & \mathbf{0} \\ \mathbf{0} & \mathbf{D}_f^+ \end{bmatrix} \tag{3.12}$$

and

$$\mathbf{D}^- = \begin{bmatrix} D_{rl^-} & \mathbf{0} \\ \mathbf{0} & \mathbf{D}_f^- \end{bmatrix} \tag{3.13}$$

The dynamic stiffness matrix for the complete infinite beam, written in a local coordinate system, is

$$\mathbf{D_{loc}} = \begin{bmatrix} \mathbf{D}^+ & \mathbf{0} & \mathbf{0} \\ \mathbf{0} & \mathbf{D}_{FFE} & \mathbf{0} \\ \mathbf{0} & \mathbf{0} & \mathbf{D}^- \end{bmatrix} \tag{3.14}$$

The assembled local DSM is a 12-by-12 matrix. We can write the matrix tranformation from local coordinate systems to global coordinate system using the matrix

$$\mathbf{C} = \begin{bmatrix} \mathbf{I} & \mathbf{0} \\ \mathbf{I} & \mathbf{0} \\ \mathbf{0} & \mathbf{I} \\ \mathbf{0} & \mathbf{I} \end{bmatrix} \tag{3.15}$$

where $\mathbf{I}$ is a 3 by 3 identity matrix. Hence the *global dynamic stiffness matrix* is

$$\mathbf{D_{glob}} = \mathbf{C}^T * \mathbf{D_{loc}} * \mathbf{C} \tag{3.16}$$

The *global dynamic flexibility matrix* is the inverse of the dynamic stiffness matrix

$$\mathbf{H} = (\mathbf{D_{glob}})^{-1} \tag{3.17}$$

3.4 Estimation of reflection and transmission coefficients

The aim of the work is to estimate reflection and transmission coefficients in presence of a change in the structure. To estimate these coefficients for a delaminated beam, we consider a wave propagating in positive-x direction from the left-hand semi-infinite beam; this wave is incident on the delamination, as shown in Fig.(3.3).

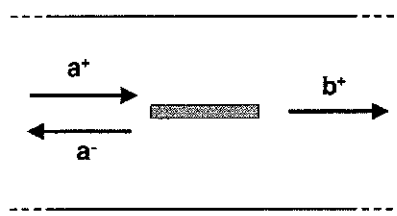

Figure 3.3: Reflection and transmission at the delamination.

The applied method (reference [1]) uses superposition to evaluate the coefficients. The first step of the method is called *blocked case*: referring to Fig.(3.4), if we consider a propagating wave incident on the fixed end of a semi-infinite beam, we can calculate the internal force due to the propagating wave. To evaluate the internal force, named the *blocked force*, we apply Love rod theory and Timoshenko theory for longitudinal and flexural waves. At first we evaluate the reflection coefficient for longitudinal and flexural waves.

As seen in subsection (1.2.3), the reflection coefficent for longitudinal waves is $r_l = -1$. For flexural waves, we write displacement w and rotation ψ (1.74) in matrix form as

$$\left\{ \begin{array}{c} w \\ \psi \end{array} \right\} = \left[\begin{array}{cc} e^{-ik_A x} & e^{-k_B} \\ R_A e^{-ik_A x} & R_B e^{-k_B} \end{array} \right] \left\{ \begin{array}{c} A^+ \\ A_n^+ \end{array} \right\} + \left[\begin{array}{cc} e^{ik_A x} & e^{k_B} \\ -R_A e^{ik_A x} & -R_B e^{k_B} \end{array} \right] \left\{ \begin{array}{c} A^- \\ A_n^- \end{array} \right\} \tag{3.18}$$

Equating them to zero at $x = 0$ gives

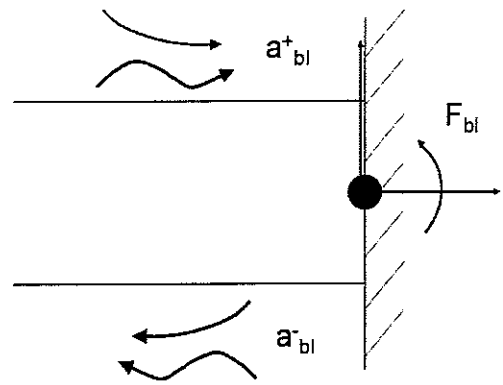

Figure 3.4: Blocked case

$$\left\{ \begin{array}{c} 0 \\ 0 \end{array} \right\} = \mathbf{Z}\mathbf{a}_{bl}^{+} + \mathbf{Y}\mathbf{a}_{bl}^{-} \tag{3.19}$$

where $\mathbf{a}^{+} = \{A^{+}A_n^{+}\}^T$, $\mathbf{a}^{-} = \{A^{-}A_n^{-}\}^T$ and

$$\mathbf{Z} = \left[\begin{array}{cc} e^{-ik_A x} & e^{-k_B} \\ R_A e^{-ik_A x} & R_B e^{-k_B} \end{array} \right] \tag{3.20}$$

$$\mathbf{Y} = \left[\begin{array}{cc} e^{ik_A x} & e^{k_B} \\ -R_A e^{ik_A x} & -R_B e^{k_B} \end{array} \right] \tag{3.21}$$

The reflection coefficent matrix for flexural waves is thus

$$\mathbf{r}_f = \mathbf{Y}^{-1}\mathbf{Z}\mathbf{a}^{+} \tag{3.22}$$

The full matrix of reflection coefficients is then

$$\mathbf{r}^{blo} = \left[\begin{array}{cc} r_l & \mathbf{0} \\ \mathbf{0} & \mathbf{r}_f \end{array} \right]$$

The blocked force for an incident longitudinal wave, according to the Love rod theory, for an orthotropic laminate beam, referring to subsection (1.6.4), is

$$\mathbf{F}_l^{blo} = -2ik_l \left(ES\right)^* + 2ik_l\omega^2 \left(\rho J\right)^* \tag{3.24}$$

For flexural waves, according to equations (1.74), (1.85) and (1.89), we can write

$$\mathbf{F}_f^{blo} \left\{ \begin{array}{c} T \\ M \end{array} \right\} = (\mathbf{M}_1 + \mathbf{M}_2 \mathbf{r}_{flex})\, \mathbf{a}_{blo}^{+} \tag{3.25}$$

where

$$\mathbf{M}_1 = \left[\begin{array}{ll} bA_{44}\kappa\,(-R_A - ik_A) & bA_{44}\kappa\,(-R_B - k_B) \\ bD_{11}\,(-ik_A R_A) & bD_{11}\,(-k_B R_B) \end{array} \right] \tag{3.26}$$

and

$$\mathbf{M}_2 = \left[\begin{array}{ll} bA_{44}\kappa\,(-R_A - ik_A) & bA_{44}\kappa\,(-R_B - k_B) \\ bD_{11}\,(-ik_A R_A) & bD_{11}\,(-k_B R_B) \end{array} \right] \tag{3.27}$$

The complete *blocked force matrix*, relating the nodal forces at the six nodal semi-infinite SE DOFs for each of the possible incident waves, is given by

$$\mathbf{F}^{blo} = \left[\begin{array}{lll} F_l^{blo} & 0 & 0 \\ 0 & \mathbf{F}_f^{blo}(1,1) & \mathbf{F}_f^{blo}(1,2) \\ 0 & \mathbf{F}_f^{blo}(2,1) & \mathbf{F}_f^{blo}(2,2) \\ 0 & 0 & 0 \\ 0 & 0 & 0 \\ 0 & 0 & 0 \end{array} \right] \tag{3.28}$$

In the second step of the method we apply the blocked force, with opposite sign, to the node between the left-hand semi-infinite beam and the FE model, as shown in Fig.(3.5).

The resulting wave amplitudes $\mathbf{a}_{se}^{-}$ and b_{se}^{+} are related to the nodal forces by

$$\mathbf{H} \left\{ \begin{array}{c} -\mathbf{F}^{blo} \\ \mathbf{0} \end{array} \right\} = \left[\begin{array}{c} \mathbf{Y}\mathbf{a}_{se}^{-} \\ \mathbf{Z}\mathbf{b}_{se}^{-} \end{array} \right] \tag{3.29}$$

The superposition of the first and the second cases (blocked force due to the fixed end and the application of the opposite of the blocked force) results in the net nodal force being zero. We obtain

$$\mathbf{0} - \mathbf{H} \cdot \mathbf{F}^{blo} = \left[\begin{array}{c} \mathbf{Z}\mathbf{a}^{+} + \mathbf{Y}\left(\mathbf{a}_{se}^{-} + \mathbf{a}_{bl}^{-}\right) \\ \mathbf{Z}\mathbf{b}_{se}^{+} \end{array} \right] \tag{3.30}$$

The reflection and transmission coefficents are thus given by

$$\mathbf{r} = -\mathbf{Y}^{-1} \left\{ \mathbf{H}_1 \mathbf{F}^{bl} + \mathbf{Z} \right\} \tag{3.31}$$

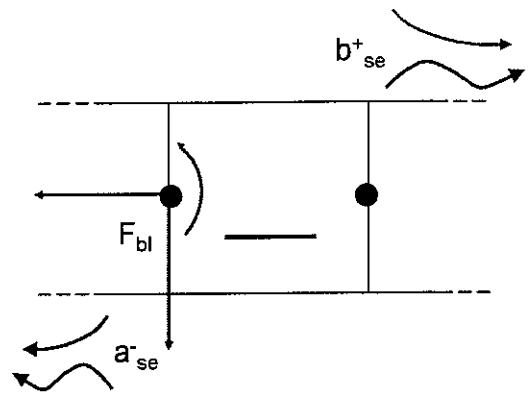

Figure 3.5: Blocked case

$$t = -\mathbf{Z}^{-1}\mathbf{h_2}\mathbf{F}^{bl} \tag{3.32}$$

where

$$\mathbf{H_1} = \begin{bmatrix} H_{11} & H_{12} & H_{13} \\ H_{21} & H_{22} & H_{23} \\ H_{31} & H_{32} & H_{33} \end{bmatrix} \tag{3.33}$$

and

$$\mathbf{H_2} = \begin{bmatrix} H_{41} & H_{42} & H_{43} \\ H_{51} & H_{52} & H_{53} \\ H_{61} & H_{62} & H_{63} \end{bmatrix} \tag{3.34}$$

Chapter 4

Numerical results

4.1 General aspects

In this chapter we apply the method developed earlier to estimate the reflection and transission coefficient of a laminated infinite beam with a delamination. We show how the Finite Element model for the delaminated region is built. Numerical results are shown, considering different stacking sequences of the beam and different lengths of the delamination and position between layers, in order to establish a relation between these parameter and the values of the reflection and trasmission coefficients.

4.2 Finite Element model of the delaminated region

Ansys 7.1 was used to model the damaged area. The structure is modelled using plane elements (Plane42) with four nodes and two degrees of freedom at each node (translation in x and z direction), using the *plane stress option*. The element size is 0.25 mm by 0.25 mm.

The modelled structure is an 8-layer laminate beam of carbon fibers and epoxy matrix; the density of the composite material is $\rho = 1496\ kg/m^3$ and the elastic properties of the material are shown in table (4.1).

E $[Pa]$	$E_1 = 1.11e11$	$E_2 = 7.857e9$	$E_3 = 7.857e9$
ν	$\nu_{12} = 0.3344$	$\nu_{13} = 0.0.3344$	$\nu_{23} = 0.345$
G $[Pa]$	$G_{12} = 3.292e9$	$G_{13} = 2.44e9$	$G_{23} = 3.292e9$

Table 4.1: Material Elastic Properties

Here, direction 1 is along the fibres, direction 2 is perpendicular to the fibres in the plane of the laminate and direction 3 is the axis out of the plane. The dimensions of the FE modelled beam are shown in Fig.(4.1). For all the

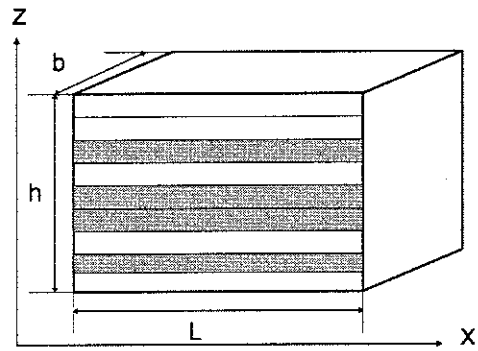

Figure 4.1: FE model of the delaminated region

numerical cases we have considered the dimensions are: $L = 50\ mm$, $h = 2$ mm and $b = 2\ mm$.

4.3 Numerical results

In order to evaluate the reflection and transmission coefficients, analytical models of the Spectal Elements of the semi-infinite beams were implemented in Matlab. Using a Matlab code we join the two SE with the FE of the damaged region, as described in section (3.3).

4.3.1 Undamaged beam

The stacking sequence of the considered undamaged beam is $[0/90/90/0]_S$. In this case, because of the symmetry of the lamination, there is no coupling between bending and torsion; if the lamination is not symmetrical, incident waves of one type scatter into waves of all types, e.g. incident longitudinal waves give bending waves as well as longitudinal waves.

The magnitudes of the longitudinal reflection and transmission coefficients for this case are shown in Fig.(4.2) and Fig.(4.3); the coefficients are plotted as a function of h/λ_A, where h is the height of the beam and λ_A is the Timoshenko bending wavenumber. As expected, the values of the reflection and transmission coefficients in the absence of delamination are very close to zero and one, respectively, for low values of h/λ_A.

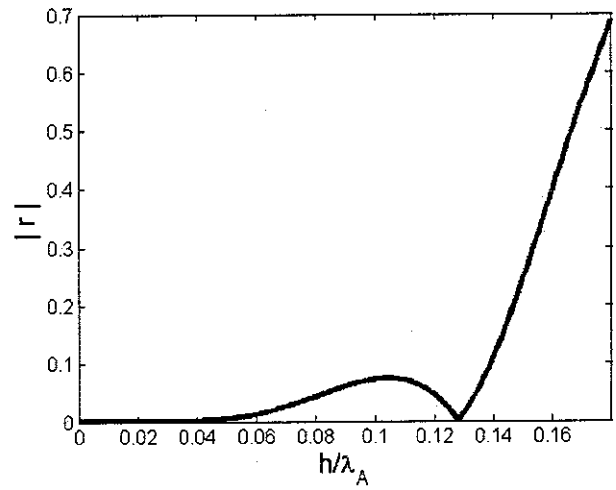

Figure 4.2: Magnitude of longitudinal reflection coefficient: undamaged beam

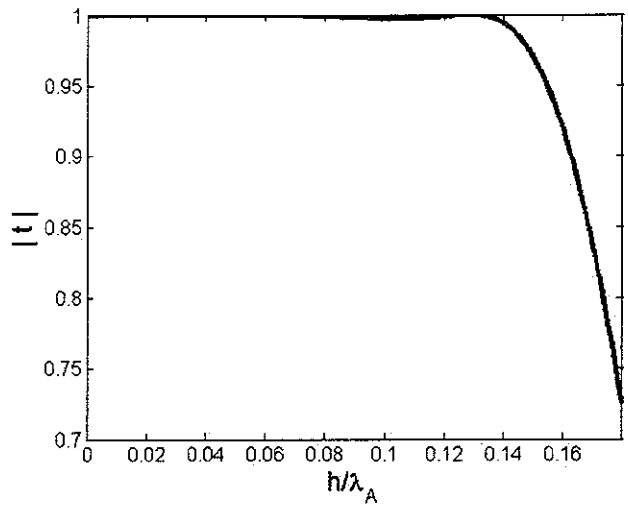

Figure 4.3: Magnitude of longitudinal transmission coefficient: undamaged beam

For values of frequency such that $(h/\lambda_A > 0.12)$ there are very substantial errors, because the method uses two models (the finite element model for the damaged area and the spectral element for the semi-infinite rods) with different distributions of displacements and, consequently, different distributions of stress. The flexural reflection and trasmission coefficients for the same undamaged beam are shown in Fig.(4.4) and Fig.(4.5)

It is possible to notice the effect of the non-perfect junction between the two semi-infinite beams modelled with the SE and the finite beam modelled using FE: to join them it is necessary to make some approximations, such as the reduction the number of nodes and degrees of freedom for each node. This junction causes partial reflection of the incident wave that is clearly visible if we consider high frequencies: in fact, as shown in the considered picture, the value of the reflection coefficient grows as the ratio (h/λ_A) grows. We can notice a periodic trend of the value of the coefficent, due to the continuous reflection of the waves between the boundaries of the beam modelled with FE. The position of peaks depends on the length of the FE modelled beam and the wavelength. To minimise this effect it is necessary to use a more exact FE model and to develop Spectal Elements based on higher order theories.

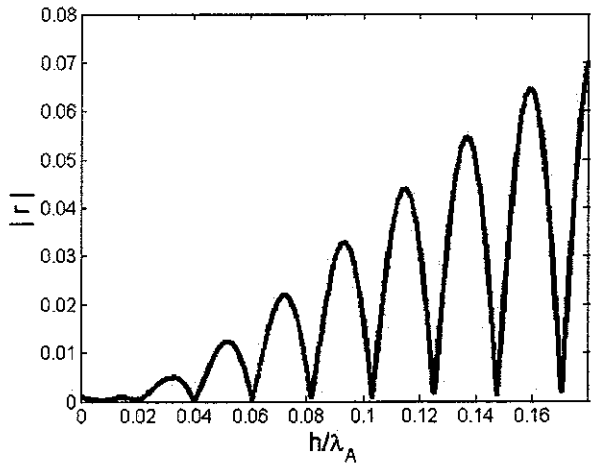

Figure 4.4: Magnitude of flexural reflection coefficient: undamaged beam

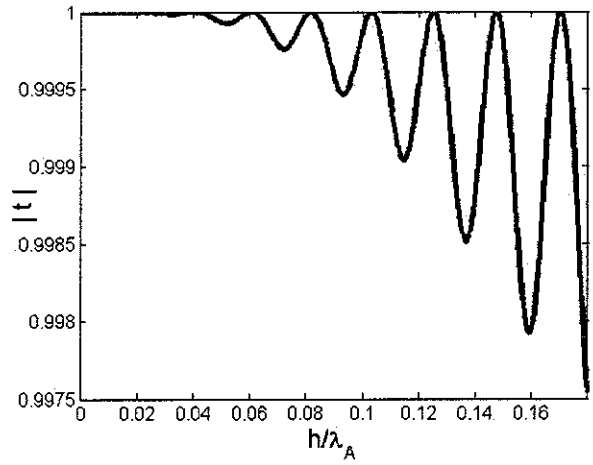

Figure 4.5: Magnitude of flexural transmission coefficient: undamaged beam

Subsequent figures will be plotted cosidering the ratio $h/\lambda_A < 0.1$, in order to have the maximum error close to 8 per cent on the value of the reflection coefficient for axial waves.

4.3.2 Delaminated beam

In order to evaluate the effect of the presence of the delamination on an incident flexural incident wave we have plotted in Fig.(4.6) and Fig.(4.7) the flexural reflection and transmission coefficients for the damaged and undamaged cases. The delamination of length $L = 20\ mm$ in this case is in the centre of the FE modelled beam, between the fourth and the fifth layer.

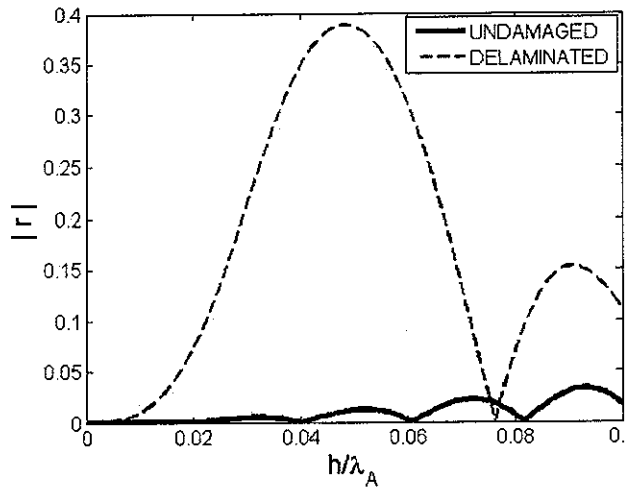

Figure 4.6: Magnitude of flexural reflection coefficient: delaminated beam

The coefficients for the undamaged beam and for the delaminated one are very different: the effect of the reflection due to the non-perfect junction between the models can be neglected if compared with the effect of the delamination. The longitudinal reflection and transmission coefficients are obtained considering the longitudinal waves due to an incident longitudinal wave. These coefficients in this case are the same as those for damaged and the undamaged case because, for a delamination at the centre of the beam, symmetry implies that there is no discontinuity.

4.3.3 Various delamination lengths

[!h] Flexural reflection and transmission coefficients for various lengths of the delamination, are shown in Fig.(4.8) and Fig.(4.9). We have considered

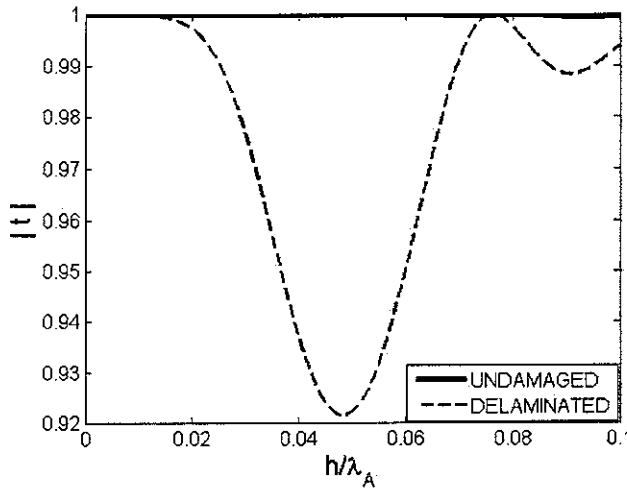

Figure 4.7: Magnitude of flexural trasmission coefficient: delaminated beam

delamination of length $L = 20\ mm$, $L = 30\ mm$, $L = 40\ mm$, between the fourth and the fifth layers.

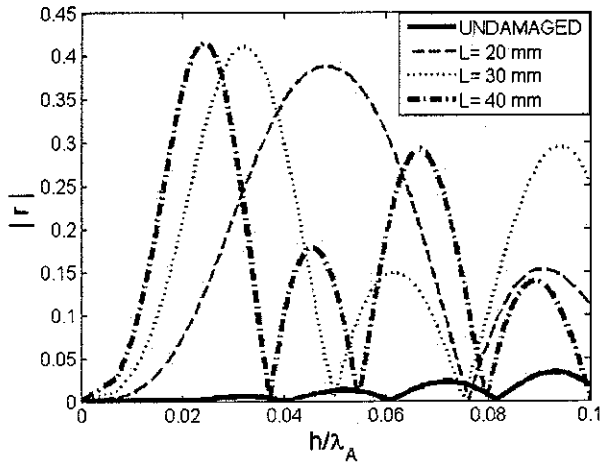

Figure 4.8: Magnitude of flexural reflection coefficient: delaminations of various lengths

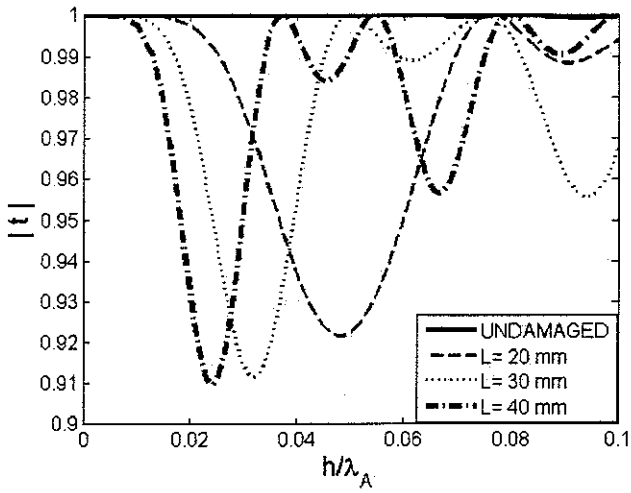

Figure 4.9: Magnitude of flexural transmission coefficient: delaminations of various lengths

It is possible to notice that as the length of the delamination gets larger, the first peak of the reflection coefficient occurs at a low value of h/λ_A. This is because it arises as a result of interference effects, which depend on the length of the delamination. Delamination shifts in the negative x direction. Another way to visualise the effect of the length of the delamination is to plot the coefficients against the ratio $(k_A L_{del})/(2\pi)$,where k_A is the wavenumber and L_{del} is the length of the delamination, as shown in Fig.(4.10) and Fig. (4.11). From these figures we can notice that the first peak occour approximately at the same frequency, varying the length of the delamination. Therefore we can conclude that, because the effect of the delamination is the introduction of a reflection of waves at its end, the first peak will be the result of this reflection. The following peaks are the result of the interferences between the reflected waves and they occur at different frequencies, depending on the length of the delamination that causes them.

We consider again delaminations of various lengths, changing the layers between which the delamination lies. The values of the coefficients calculated for a delamination between the second and the third layer are shown in Fig.(4.12) and Fig.(4.13).

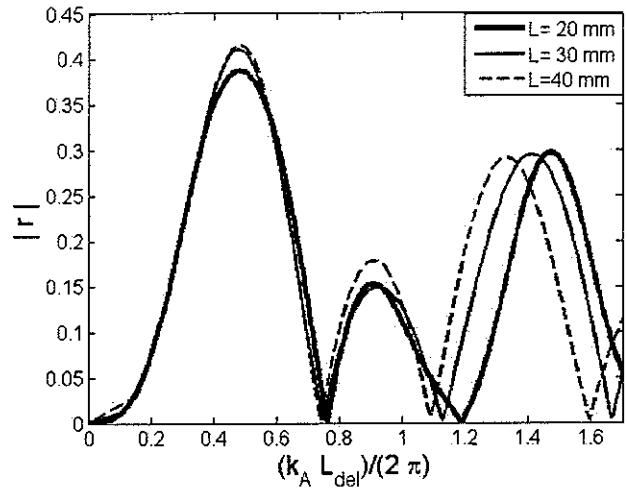

Figure 4.10: Magnitude of flexural reflection coefficient: delaminations of various lengths between the fourth and the fifth layer

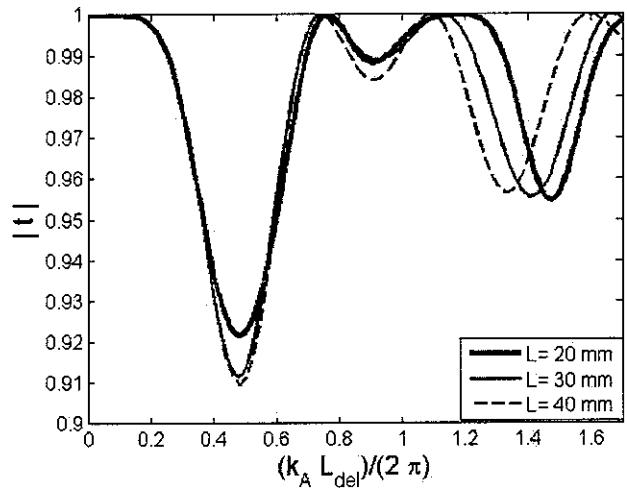

Figure 4.11: Magnitude of flexural transmission coefficient: delaminations of various lengths between the forth and the fifth layer

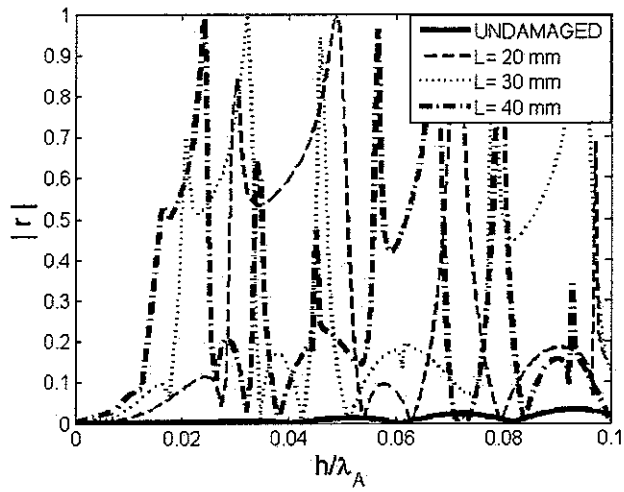

Figure 4.12: Magnitude of flexural reflection coefficient: delaminations of various lengths between the second and the third layer

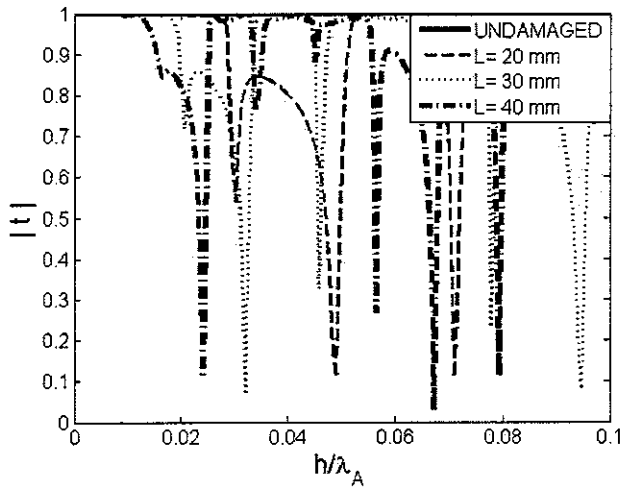

Figure 4.13: Magnitude of flexural transmission coefficient: delaminations of various lengths between the second and the third layer

It is possible to notice that the values of the reflection and transmission coefficients, in this case, are very different from the values in the undamaged case. There is not a regular trend of the coefficient as in the previous case and the plots present many peaks. The different behaviour is probably due to the effect of the bending-extensional coupling. The beam has, in fact, a symmetric stacking sequence; as a consequence, there is not coupling between bending and extension. The delamination between the second and the third layer divide the laminate into two non-symmetric sublaminates, the consequence is the presence of the coupling. The presence of the coupling can be clearly shown considering the off-diagonal terms of the matrices of the reflection and transmission coefficients. In the Fig.(4.14) the amplitude of the reflection coefficient r_{12} for a delamination of length $L = 20\ mm$ between the fourth and the fifth layer and the second and the third layer are shown. The coupling term r_{12} gives the amplitude of the reflected bending wave due to an incident longitudinal wave.

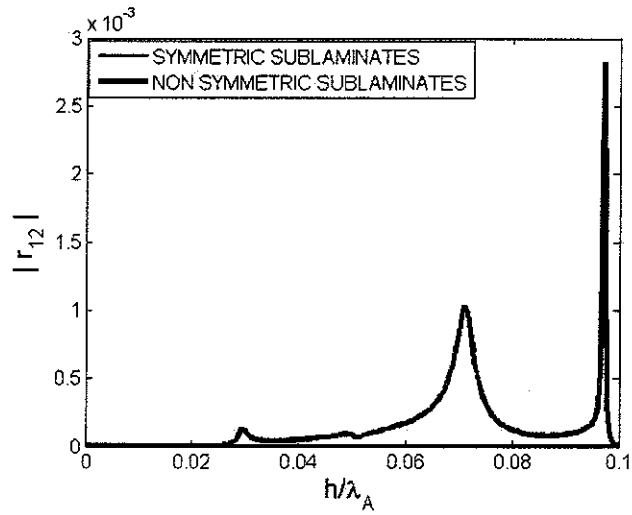

Figure 4.14: Coupling term: reflection coefficient r_{12}

If the resulting sublaminates are symmetric r_{12} is negligible (no coupling); if the sublaminates are not symmetric, r_{12} generally increases with frequency.

4.3.4 Various positions of the delaminations between layers

The third considered case presents beams with delaminations of length $L = 20\ mm$, with different position between layers; the results are shown in Fig.(4.15) and Fig.(4.16).

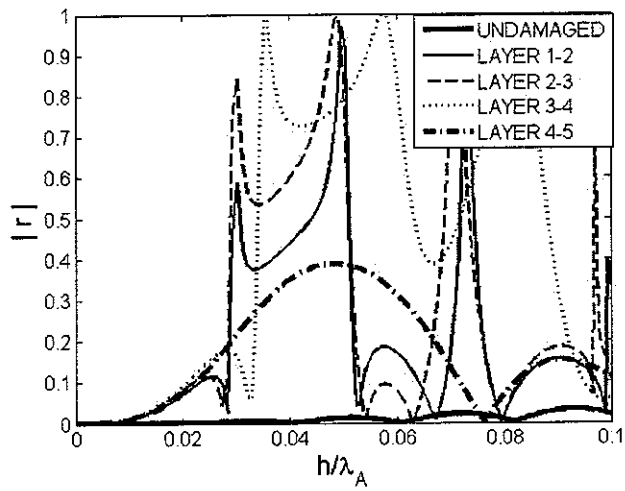

Figure 4.15: Magnitude of flexural reflection coefficient: various positions between layers

The fourth case considers a beam with stacking sequence, $[0/90/0/90]_S$. The reflection and transmission coefficients for different position of the delamination between layers are shown in Fig.(4.17) and Fig.(4.18).

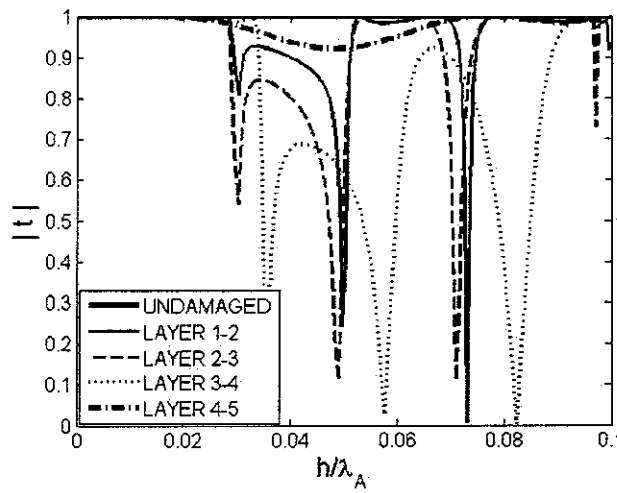

Figure 4.16: Magnitude of flexural transmission coefficient: various positions between layers

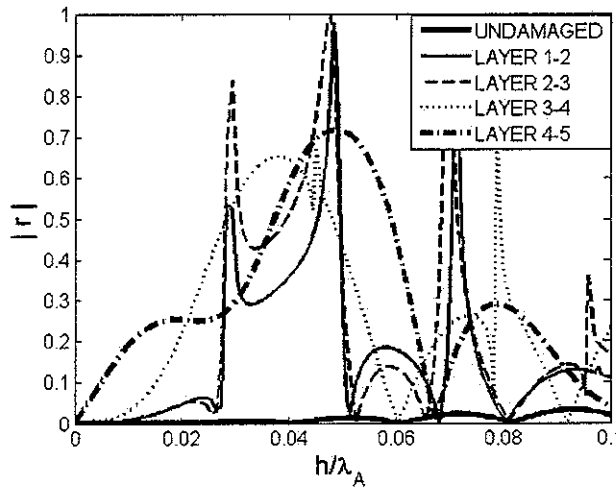

Figure 4.17: Magnitude of flexural reflection coefficient: various positions between layers

Comparing the former figures with Fig.(4.15) and Fig.(4.16) it is clearly visible that reflection and transmission coefficients are not strongly affected by changing the stacking sequence.

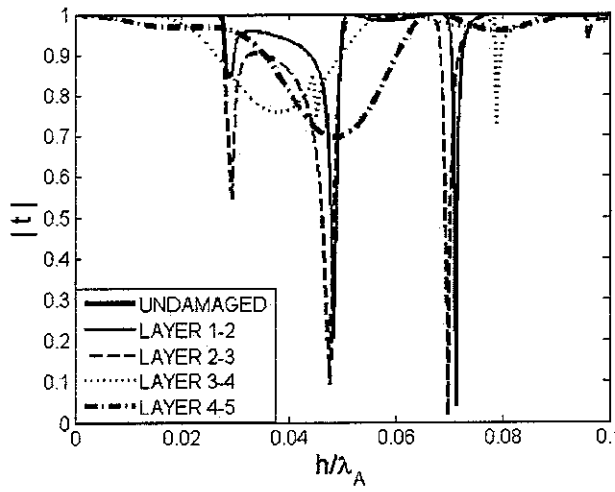

Figure 4.18: Magnitude of flexural transmission coefficient: various positions between layers

Conclusions

The described work presents the evaluation of the reflection and the transmission waves due to the presence of a delamination in a laminated multilayered composite beam. The infinite beam has been modelled joining the Finite Element model of the delamainated area and two Spectral Element models of semi infinite beams. The Spectral Element models are developed using elementary rod theory, Love rod theory, Euler-Bernoulli and Timoshenko theories.

The presence of the delamination is evaluated comparing the amplitude of the reflection and transmission coefficients of an undamaged and a delaminated beam. It is well-known, in fact that, for an undamaged beam the incident wave is totally transmitted; the presence of the delamination causes a partial reflection (and a consequent partial transmission) of the incident wave. The coefficients have been evaluated considering incident bending waves; the longitudinal coefficients do not point out the presence of the defect. The non-perfect junction between models influences the numerical results; in order to minimize this effect we consider a limited frequency range.

The length of the delamination and its position between layers influence the value of the reflected and transmission coefficients. If we divide a symmetric laminate into two non-symmetric sublaminates, the off-diagonal terms of the reflection and trasmission matrices are not negligible because of the coupling effect between longitudinal and flexural waves.

Future work should minimise the effect of the junction between models and to develop Spectral Elements according to higher order laminate theories and evaluate if this is a suitable basis for a delamination detection technique.

Bibliography

[1] S.P. Shone, B.R. Mace, T.P. Waters. *Reflection and Transmission Coefficients using the Spectral Element Method: Application to crack modelling in beams.* Proceedings of Institute of Acoustics Spring Conference, Institute of Sound and Vibration Research, Southampton, UK, 29-30 March 2004.

[2] S.P. Shone, B.R. Mace, T.P. Waters. *Reflection of Waves from Cracks in Beams.* Proceedings of ISMA 2004, International Conference on Noise and Vibration Engineering, Leuven, 2004.

[3] S.P. Shone, B.R. Mace, T.P. Waters. *A Combined Finite and Spectral Element Approach to Wave Scattering in a Cracked Beam: Modelling and Validation.* Proceedings of DAMAS 2005, Gdansk, 2005.

[4] Wave Motion in Elastic Solids, Karl F. Graff. *Dover Publications, Inc.* New York, 1991.

[5] A.E.H. Love. *A Treatise on the Mathematical Theory of Elasticity.* Cambridge University Press, 1959.

[6] J.N. Reddy. *Mechanics of Laminated Composite plates and Shells-Theory and Analysis.* 2nd Edition, CRC Press, 2004.

[7] J.F. Doyle. *Wave Propagation in Structures: Spectral analysis using Fast Discrete Fourier Transform.* 2nd Edition, Springer, 1997.